NATIONAL UNIVERSITY of SCIENCE and TECHNOLOGY

POLITEHNICA BUCHAREST

DOCTORAL SCHOOL of ELECTRICAL ENGINEERING

EXTENDED ABSTRACT
Ph. D. THESIS

Applications of electrical engineering in neuroscience – cortical stimulation by electromagnetic induction

Ph. D. Student:

Drd. Chris Maria CIOCĂZANU

Ph. D. Supervisor:

Prof. dr. ing. Mihaela MOREGA

BUCHAREST

2026

Contents

1 Introduction. General information about electromagnetic induction stimulation

1.1 Choosing the topic and its placement in the field of electrical engineering

The spectacular evolution of medical intervention technologies / procedures / methods that call on advanced physical principles is currently experiencing a notable development oriented towards new medical engineering applications; ideas for new clinical technologies are constantly emerging and they are put into practice with the help of modern equipment of high precision and safety (for the patient and the medical staff). Engineering has a very important role, because it provides the practical application framework for physical principles and the necessary technical infrastructure – equipment with electrical, electronic, mechanical components, advanced substances and materials. In addition to the facilities offered by electrical engineering, the experience of specialists in the field is particularly appreciated in ensuring minimal risk conditions, both for patients and for medical staff involved in the application of therapies – specific electrical safety of medical equipment and control of exposure to electromagnetic emissions. In the context of medical technologies based on the exposure of the body to electromagnetic fields, specifically through the *phenomenon of electromagnetic induction*, the doctoral thesis analyzes problems related to the production of electrical stimuli and their application to neuronal cells, a procedure commonly called "magnetic stimulation". The applied aspects addressed in the thesis refer to cortical stimulation, generically called *transcranial magnetic stimulation*; in the specialized literature, the acronym TMS is widely used from the English name - **Transcranial Magnetic Stimulation**, an acronym also adopted in this work.

The research program addressed falls within the field of electrical engineering through the following aspects:

- The procedure for stimulating excitable tissues (especially neuronal cells) by electromagnetic induction is a typical application of the theory of electromagnetism: the production of the inductive magnetic field has as its theoretical support the law of the magnetic circuit, the basis for the production of the intratissue stimulus are the law of electromagnetic induction and the law of electrical conduction. Moreover, for the understanding and quantitative analysis, electrical circuit models associated with the structure and electro-physiology of neuronal cells and the connections between them are used.
- The equipment used is built with electrical and electronic components (inductive current generation circuit, inductor coil).

- Analysis of the circuit problem to establish the waveform of the current pulse and the analysis of magnetic field problems (with the application of finite element numerical analysis and implementation in Comsol Multiphysics) are approaches typically used in electrical engineering. Also, the theory of electromagnetism is applied for post-processing of solutions and determination of derived quantities, both for the main stimulation effect (induced electric field intensity, induced current density) and for the evaluation of possible side effects (electro-thermal effects – heating of the applicator or dangerous heating of tissues, such as the lens).
- Last but not least, the operation of typical equipment in transcranial magnetic stimulation (TMS) presents potential risks due to the electrical and magnetic parameters with which it operates (current intensities through the applicator coils of the order of kA and inductive magnetic fields of 2.5 – 3 T in the immediate vicinity of the coil) through possible effects of electromagnetic interference with equipment in the area (therapeutic equipment, active implants or communication devices). Interferences and their effects can be estimated, monitored and prevented by methods specific to electrical engineering. The proper functioning of electrical and electronic therapeutic equipment is ensured by compliance with specific electrical safety and electromagnetic immunity standards.

1.2 Clinical utility of medical magnetic stimulation procedures

After testing some neuromodulation technologies in the clinical setting (neurology, psychiatry) and evaluating their effectiveness and accessibility (Barker, 1985), the implementation of transcranial magnetic stimulation (TMS) in medical practice expanded significantly only after 2008, when this technique received approval from the US Food and Drug Administration (FDA), the internationally recognized authority for the regulation of health devices and treatments (Cohen, 2022). Initially, the FDA approved TMS as a therapy for the treatment of major depression in adults, using the Neurostar TMS system, which quickly became a successful commercial device (DEN070003) (Cohen, 2022). After 2008, numerous TMS-based protocols were developed, including classical, repetitive stimulation (rTMS), deep stimulation, and neuronavigation-guided stimulation, for the treatment of psychiatric and neurological conditions. Recently, psychotherapists have also begun to integrate TMS into neurofeedback protocols, especially since both specialists and patients appreciate the non-invasive nature of the method (Kumsa, 2018). In addition to the initial devices, commercial systems have been developed and rapidly approved internationally to expand the applicability of TMS and improve the technical aspects of the medical procedure (Gutierrez, 2022). For example, a study of neuroengineering devices produced in the USA identified eight systems specifically designed for electrical stimulation, which obtained FDA approval in a relatively short period of time, between 2013 and 2018 (Ereifej, 2019). A synthesis of the technological progress of clinical TMS devices approved by the FDA is presented by (Cohen, 2022), illustrating the rapid expansion of this technology in the field of mental health, based on principles and equipment from electrical engineering.

2 Transcranial magnetic stimulation, application of electromagnetism

Transcranial magnetic stimulation (TMS) is a non-invasive method that uses a variable magnetic field to create an induced current inside the body, which can stimulate neuronal formations in the cerebral cortex. TMS works on the principle of electromagnetic induction, so it uses inductor coils (coils with a variable current) to produce a variable magnetic field (the same waveform as the current through the coils) in the intervention area; the inductive magnetic field is produced due to the conduction current (with current density **J**) that flows through the coils of the inductor, according to the *law of the magnetic circuit* (rot $\mathbf{H} = \mathbf{J}$).

By electromagnetic induction, an induced electric field is created in the volume of tissue impacted by the variable magnetic field. The magnitude of the induced electric field intensity (Ei) depends on the magnitude of the induction **B** (respectively the intensity **H**) of the inductive magnetic field and on its frequency of variation in time. The occurrence of the induced electric field is quantified based on the *law of electromagnetic induction*, namely the pulsation induction (rot $\mathbf{E_i} = - \partial\mathbf{B}/\partial t$) without the electrical properties of the tissue affecting the magnitude and distribution of the induced electric field $\mathbf{E_i}$; instead, the density of the stimulation current, justified by the *law of electrical conduction* ($\mathbf{J_i} = \sigma\ \mathbf{E_i}$), is determined not only by the magnitude of $\mathbf{E_i}$, but also by the material property, the electrical conductivity of the tissue σ. Tissues have relatively good electrical conductivity, so that under the incidence of the induced electric field an induced electric current is formed (electrical conduction law). This acts in the area of excitable cells as an electrical stimulus (stimulation current); Under these conditions, it is explained why the stimulation (induced) current is stronger the more it is applied to a better conductive tissue environment.

The physical principle of the TMS procedure and the magnetic field theory are presented below.

Magnetic stimulation can activate peripheral nerves in a manner analogous to electrical stimulation. The applicator, consisting of an external electrical circuit, is inductively coupled to the target conductive tissue in the body, where the generated electrical currents stimulate excitable structures, especially neurons (see Figure 2.1).

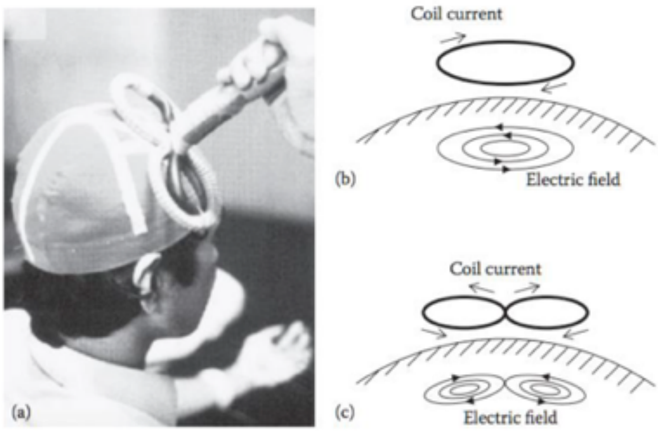

Figure 2.1 Basic principle in TMS - inductor coil positioned above the head (a) and associated diagrams of electromagnetic induction (b and c) (after Ueno and Sekino, 2016).

2.1 The production of the inductive magnetic field

The magnetic field produced at a distance r in the vicinity of a conductor carrying current i can be determined by applying the *law of the magnetic circuit*, or in its simplified form *Ampère's theorem*, which includes only the effect of the conduction current. The magnetic field generated around the conductor is expressed by the intensity **H** or by the induction **B**, between the two quantities being stable by the *material law* $\mathbf{B} = \mu\,\mathbf{H}$, knowing that in the case of TMS, the media are non-magnetic ($\mu = \mu_0$).

2.2 Induced electric field

Commercial applicators used in TMS are generally single or double circular coils ("figure eight"), as seen in Figure 2.1 or in the studies of Klomjai (2015) and in the manufacturers' documentation. These coils are made of copper conductor with a rectangular cross-section and have a relatively low number of turns (< 20), being encapsulated in insulating material. They generate a magnetic flux with high induction values around the coils (1.5–3 T at the coil surface) and induce electric fields of 150–180 V/m in the target areas of stimulation in the brain.

For research, the literature proposes a variety of geometries and positioning of stimulation coils, such as double conical or batwing coils, or circuits distributed around the scalp, such as Halo Coil or Hesed Coil. These variants are developed according to optimization criteria such as:

- Stimulation of deeper areas of the cortex (Guadagnin, 2016; Lu and Ueno, 2015).

- More precise focusing of the stimulus (Gomez, 2020).

- Reduction of side effects, such as unwanted inhibitory effect in the proximity of stimulated areas or overheating of the coil (Zibman, 2021).

The law of electromagnetic induction, established on an experimental basis by Michael Faraday in 1831, describes how the induced electromotive tensim (induced t.e.m.), or the induced electric field, can be produced as a result of two distinct phenomena: induction by the time variation of the magnetic flux, known as *pulsation induction*, and *induction by the movement* of a receiving body (conductor, circuit, massive body, etc.) in a static magnetic field, called motion induction. The pulsation induction phenomenon is the main mechanism used in the application of magnetic stimulation, being of particular interest in the field of electrical engineering for the development of medical technologies for non-invasive stimulation of excitable tissues (neuronal, muscular, sensitive).

The equation of the *law of electromagnetic induction* for the induced electromotive force e_Γ, along the curve Γ ((Figure 2.2):

$$e_\Gamma = -\frac{\mathrm{d}\Phi_{S_\Gamma}}{\mathrm{d}t} = -\frac{\mathrm{d}}{\mathrm{d}t}\int_{S_\Gamma} \mathbf{B}\cdot\mathbf{n}\,\mathrm{d}A \tag{2.1}$$

$$e_\Gamma = e_p + e_m = -\int_{\mathbf{S}_\Gamma} \frac{\partial\mathbf{B}}{\partial t}\cdot\mathbf{n}\,\mathrm{dA} - \int_{S_\Gamma} \mathbf{n}\cdot\mathrm{rot}(\mathbf{B}\times\mathbf{v})\mathrm{dA} \tag{2.2}$$

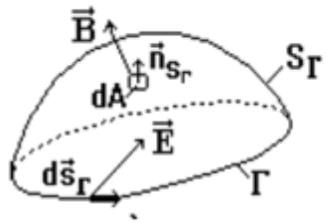

Figure 2.2 Explanatory drawing for the law of electromagnetic induction; Note: Compared to the drawing, simplified notations are adopted in the equations $\mathbf{n}=\mathbf{n}_{S\Gamma}$; $\mathbf{ds}=\mathbf{ds}_\Gamma$

By developing equation (2.1), the two terms of the induced t.e.m. are highlighted (the notations are in accordance with Figure 2.2): the term corresponding to induction by temporal variation of the field or pulsation t.e.m. e_p and the one corresponding to the phenomenon of induction by motion e_m.

The induced electric field depends on the rate of variation in time of the magnetic field and is not affected by the electrical properties of the environment, which allows the stimulus to penetrate through poorly conductive structures such as skin, skull or fat (see Figure 2.3).

The applicators used in TMS are inductive elements, ranging from simple circular coils to complex configurations (e.g. double coils "figure eight" or "Halo configurations" surrounding the head) intended for specific clinical objectives. The applicator circuit, powered by a variable current, generates a magnetic field that is freely distributed in air and tissues (non-magnetic environments), decreasing in intensity with increasing distance from the source (Ueno and Sekino, 2016).

The scheme presented in Figure 2.3 summarizes the principle of the transcranial stimulation procedure by electromagnetic induction with an applicator (here it is in the form of a simple circular coil) that generates the inductive magnetic field, variable in time as well as the current through the coils of the applicator and with a spatial distribution dependent on the configuration of the applicator. The applicator is included in an electrical circuit and placed near the head, in a convenient position for stimulation. The inductive current is generated in an *RLC* circuit by the forced discharge of the capacitor *C* on the load *RL* formed by the inductance of the applicator coil or coils and the equivalent electrical resistance in the respective circuit (see also Figure 2.4).

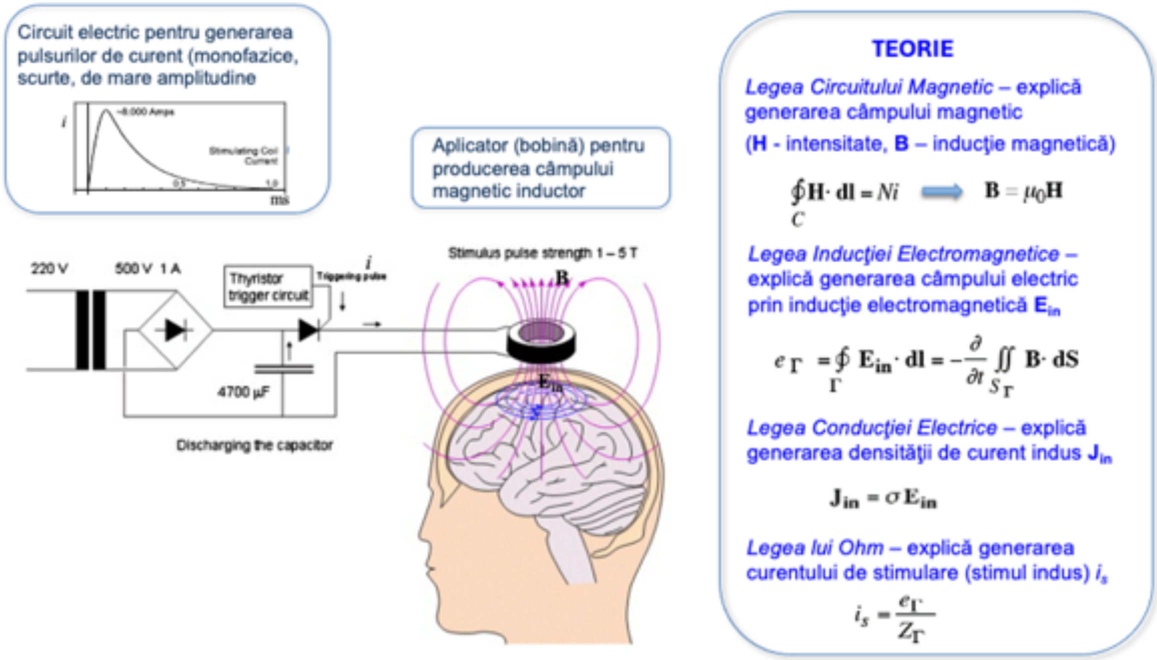

Figure 2.3 TMS principle in the absence of reaction effects – schematic representation of the electromagnetic circuit (electrical circuit taken from Malmivuo and Plonsey, 1995).

2.3 Induced current and the electrical circuit of the stimulator

For maximum efficiency of the stimulus produced by the phenomenon of electromagnetic induction, the inductive magnetic field must have a significant amplitude and a rapid variation in time, i.e. a high value of the d*B*/d*t* term in the law of electromagnetic induction, respectively of the source of this magnetic field, through the inductive current that feeds the applicator. In other words, a high value of the d*i*/d*t* term is needed. This condition is practically achieved by a pulse shape with a rapid increase towards a high amplitude of the inductive current. Usually, in TMS we work with current pulses having a peak of the order of kA and an initial increase slope of the order of 10^8 A/s. An analysis of technical solutions for generating currents with such characteristics is presented below.

Operation of the current pulse generation circuit

Figure 2.4 presents the principle of generating single-phase current pulses in a synthetic way: the electrical circuit used is schematized on the left of the figure, and the operation in the transient regime of sudden discharge of the capacitor *C* is explained by the circuit equations on the right.

Solving the circuit problem in the transient regime of capacitor discharge is synthesized in Figure 2.4 and leads to a general expression of the current obtained when the capacitor discharges, of the form:

$$i(t) = \frac{U_0}{\omega L} e^{-\alpha t} \mathrm{sh}\omega t. \tag{2.3}$$

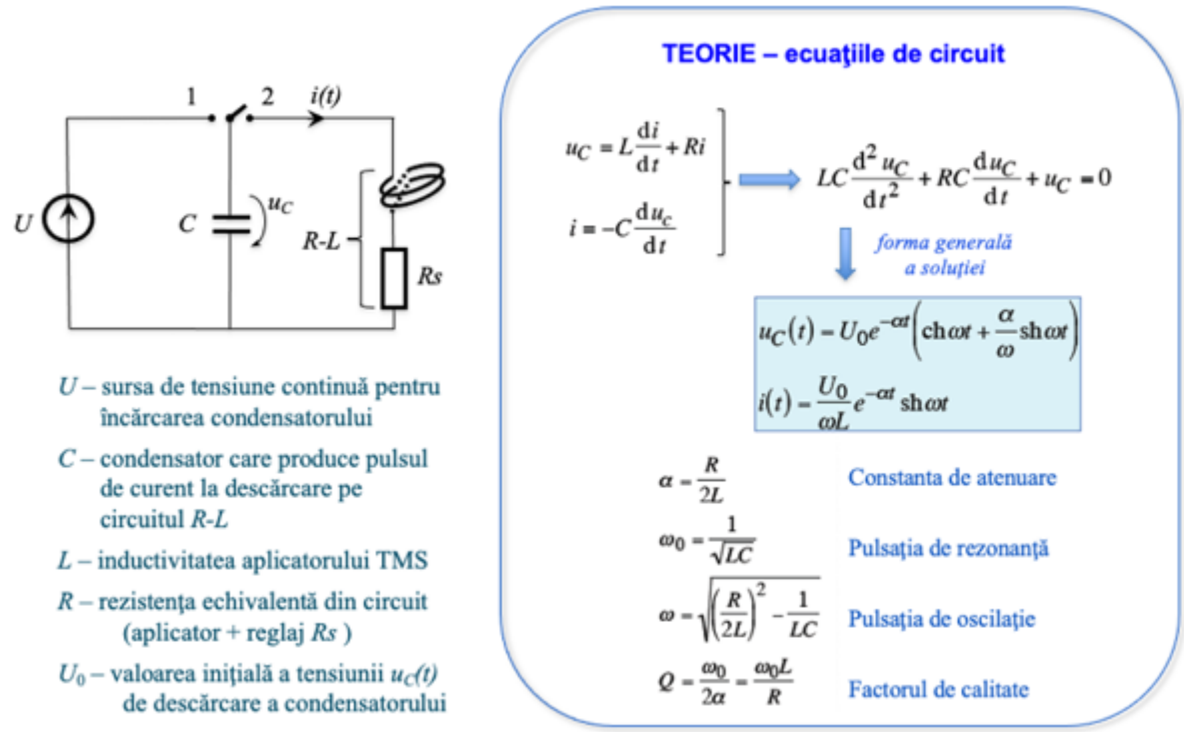

Figure 2.4 The electrical circuit for generating the pulsating current that powers the applicator; the monophasic pulses required in TMS correspond to the *critical aperiodic* transient regime (figure adapted from (Ciocăzanu, 2024)).

3 Numerical modeling for the analysis of the TMS medical procedure

Next, the TMS procedure will be analyzed through numerical simulation of the transient regime for the electric current pulse.

3.1 Objectives

The modeling and numerical analysis approach to bioelectromagnetism problems brings advantages in deepening the physical aspects of the production of the respective phenomena through aspects such as:

- the association of electrophysiological processes with general electrical and magnetic phenomena, for which electrical engineering has developed models and methods of approach;
- understanding the interactions of the electromagnetic field with tissue media having specific electrical properties can be done based on the laws of electromagnetism;
- electrical engineering offers adequate study tools - software packages adapted to the simulation of increasingly varied and sophisticated phenomena and regimes are available;
- a developed and validated numerical model can be used with minimal costs for a wide variety of particular cases;
- the development of hardware means is currently spectacular, with IT resources allowing the construction of detailed, highly accurate, realistic, personalized models;
- numerical approaches are ideally used as complementary analysis means to biomedical studies and experimental evaluations.

Numerical analysis of the electromagnetic field problem associated with transcranial magnetic stimulation (TMS) procedures capitalizes on the research experience (methods and tools) offered by electrical engineering. It can successfully replace experiments for optimizing applicator design (i.e. identifying the best correspondence between applicator design and its medical performance) and for preparing personalized therapeutic interventions through simulation.

In the study presented below, the numerical simulation of the TMS procedure is approached with the consideration of some simplifying hypotheses for the physical model adopted in the construction of the numerical model. Thus, it is considered:

- The anatomical element exposed to the TMS procedure is a representation of the human head; the shape of the head here is a realistic shape – the *Specific Anthropomorphic Mannequin* (SAM) model (described in subchapter 3.2.1 of the thesis), and the simplified structure includes a minimum of subdomains relevant for TMS – skull, brain and eyes.

- The magnetic field source – the TMS applicator – is a simple, flat circular coil, positioned symmetrically above the head (presented in subchapter 3.2.3 of the thesis).

3.2 Results

The results presented below are included in the published article (Ciocăzanu, 2024). The principle of TMS is illustrated in Figure 3.1 by tracing the main electromagnetic phenomena: (a) - generation of the inductive magnetic field by the coil through which current passes, according to the law of electromagnetic induction and (b) - production of the induced current in the exposed biological environment (the head), by electromagnetic induction.

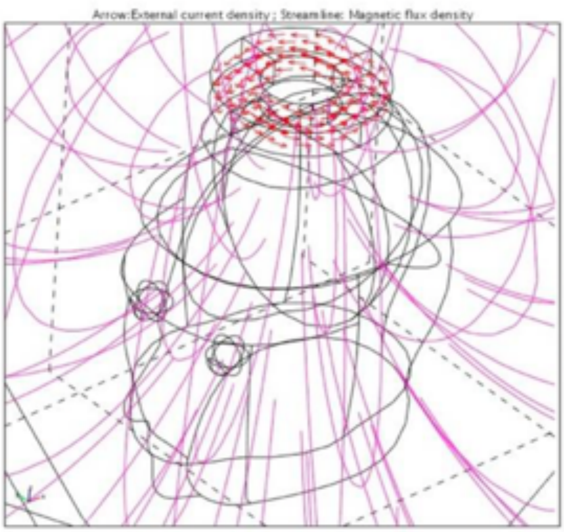

a) Current density through the coil (red arrows), magnetic induction (purple streamlines)

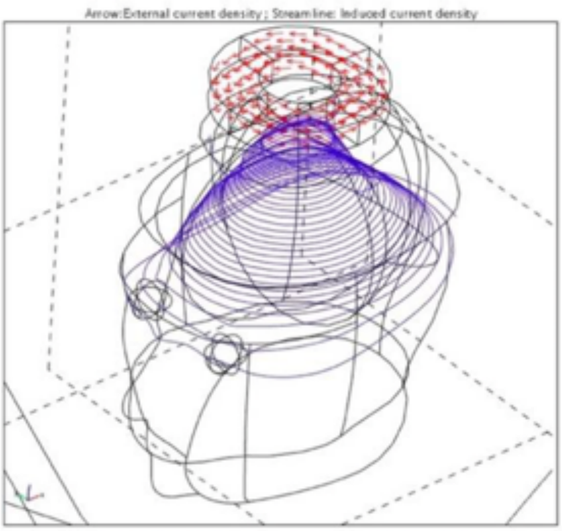

b) Current density through the coil (red arrows), current density induced in the head (blue streamlines).

Figure 3.1 Electromagnetic phenomena in TMS: (a) generation of the inductive magnetic field and (b) the effect of electromagnetic induction (induced current density).

The two images are qualitative (no representation value scale is associated), the interest being directed towards illustrating the phenomena. These illustrations also constitute a way of validating the model, by describing the simulated physical phenomena in a very clear and suggestive way.

As can be seen in both images, the current density through the coil is represented with red arrows – the current closes uniformly in the coil section (according to the adopted hypotheses). In the image on the left, a spectrum of the inductive magnetic field lines is associated (the field lines are presented in purple), and in the image on the right, a vortex-shaped spectrum of the induced current density is visible (represented in dark blue). Both spectra are represented with "stream lines" graphic options.

The localization and focusing of the stimulus are essential in TMS. The induced currents follow circular trajectories, similar to the projections of the coil inside the head, a fact confirmed by Figure 3.1.b. An inductive coupling is established between the inductor current (through the applicator coil) and the induced current (the vortex visible inside the head) (similar to the operating principle of the power transformer). The induced current paths inside the head are projections of the inductor current paths.

As a quantitative illustration, Figure 3.2 shows distributions of electromagnetic quantities along linear directions drawn in the target area inside the head. The observation lines are included in the frontal plane through the head (plane $x = 0$); they are parallel to the y -axis of the Cartesian coordinate system and to the base plane of the coil and are drawn at three distances measured on the vertical z -axis, downwards, starting from the base plane of the coil (30 mm / 40 mm / 50 mm).

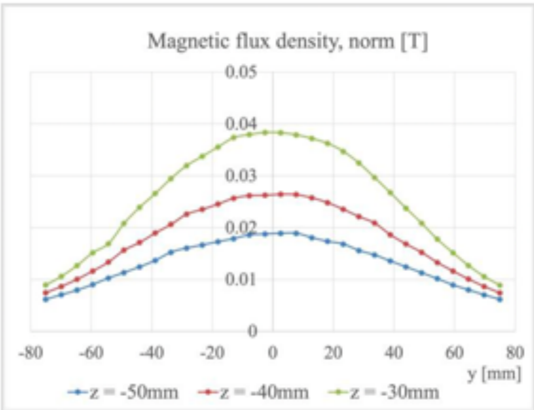

a) Magnetic induction $B(y)$

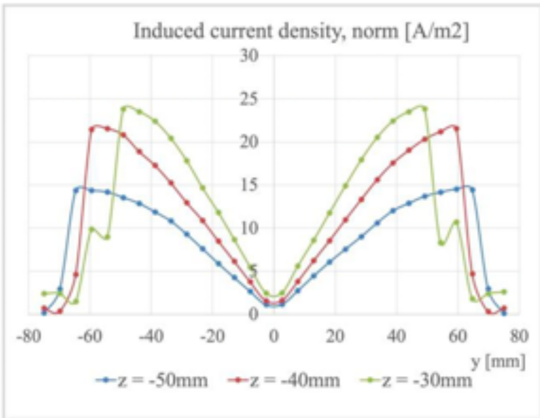

b) Induced current density $J_{in}(y)$

Figure 3.2 Distributions of TMS-specific quantities along observation lines crossing the head in the frontal plane, parallel to the coil, for time $t = 5$ μs (z -coordinates are measured from the base plane of the coil downwards: $z = -50$ mm, -40 mm, -30 mm).

In the case of a simple circular coil positioned above the head, the induced electric field and the induced current density reach maximum values in an annular region inside the head, below the coil. Of course, the amplitude values of the induced currents decrease with increasing distance from the inductive coil, because with distance the amplitude of the inductive magnetic field decreases; also, the current density depends on the electrical conductivity of the tissue medium where it is determined, according to the law of electrical conduction. Determinations are presented for the quantities: (a) – magnetic induction (magnetic flux density) quantity calculated by summing the vector components according to the relation $B = |\mathbf{B}| = \sqrt{B_x^2 + B_y^2 + B_z^2}$ and similarly (b) – induced current density $J_{in} = |\mathbf{J_{in}}|$.

All graphical representations are captured at the time $t = 5$ μs from the beginning of the transient regime, because for stimulation, the first moments of the triggering of the inductor current pulse (when the current increase slope is maximum) are of interest.

As expected, the distribution of induction and induced current density have symmetrical shapes with respect to the sagittal plane through the head ($y = 0$ plane), and the values decrease with distance from the magnetic field source, i.e. from the coil (according to the z coordinate, the highest values in the representation are for the $z = -30$ mm elevation – the green curves, i.e. at the shortest observation distance from the coil). The spatial correlation is also noticeable: the magnetic induction is maximum on the coil axis ($y = 0$) and decreases towards the area under the coils, while the induced current density is minimum on the coil axis and has maximum values in the area under the coil coils.

Another interesting result is presented in Figure 3.3 and concerns the waveforms of the same fundamental electromagnetic quantities involved in TMS and how they are correlated in time - the induction of the inductive magnetic field and the induced current density - evaluated at the same point in the target area for stimulation (a specified location in the brain), for the entire 1 ms duration of the current pulse through the coil (i.e. the entire transient process studied here). The evolution of the waveform captured for the magnetic induction is synchronized with that of the induced current density. If the magnetic induction has a time variation shape similar to that of the current pulse $i(t)$ (Figure 3.3.a), the induced current density (proportional to di/dt) is maximum at the origin, then decreases to zero at $t = 0{,}1$ ms (at the moment when $B(t)$ has its peak value). Practically, stimulation occurs in the first moments of the pulse, at the maximum values of the di/dt quantity. Knowledge of the evolution over time and the synchronization between electromagnetic quantities is important for protocol design in TMS.

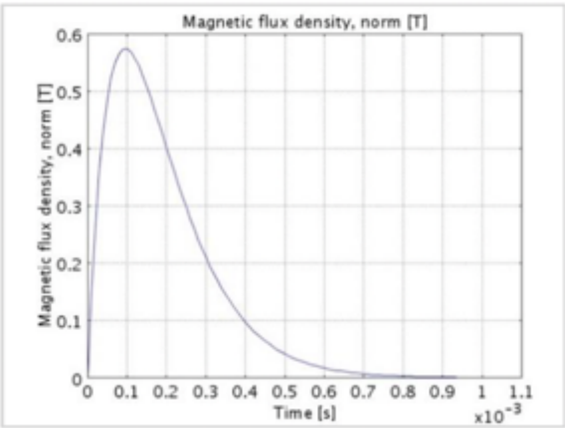

a) Magnetic induction - $B(t)$

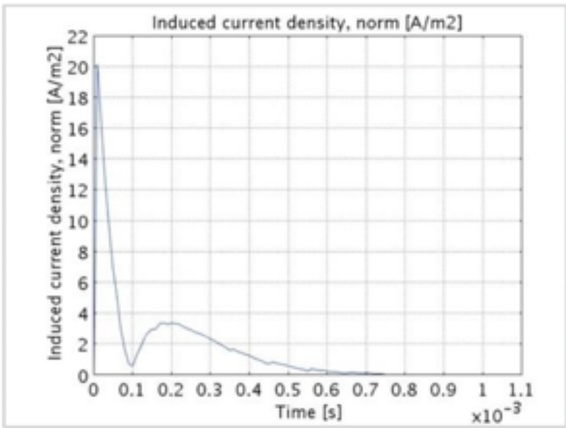

b) Induced current density $|J_{in}(t)|$

Figure 3.3 Waveforms of TMS magnitudes during a current pulse through the coil; values are averaged over a small volume of brain tissue centered under the coil (at coordinates: $x = 0$, $y =$ 30 mm, $z = -30$ mm)).

3.3 Comments and conclusions

The dependence of the active quantities in the stimulation on the electrical properties of the material can be analyzed from the equations applied in the numerical model. The magnetic induction has a waveform similar to that of the current in the coil. The direct proportionality between *i(t)*or $J_e(t)$ in this case and *B(t)* respectively is demonstrated by the law of the magnetic circuit – Ampère's theorem), the magnitude (or vector modulus) of the magnetic induction $|\mathbf{B}|$ decreases with the distance from the coil (also according to Ampère's theorem). The intensity of the induced electric field ($\mathbf{E_{in}}$) is calculated by applying the equation $\mathbf{E_{in}} = -\frac{\partial \mathbf{A}}{\partial t} - \text{grad}\, V \approx -\frac{\partial \mathbf{A}}{\partial t}$, to the solution of the magnetic field problem in **A** (solved based on eq. (2.1)), and the density of the induced current results locally, from the law of electrical conduction: $\mathbf{J_{in}} = \sigma \mathbf{E_{in}}$.

As the equations invoked here show, in non-magnetic materials and under the assumption of neglecting the magnetic reaction of the induced currents, the magnetic field is the same around the source, regardless of whether the head is present; in the same way, the electric field intensity does not depend on the presence of the head either, if the -grad *V* component is neglected (and this is a feature of the implementation of the transient regime in Comsol in the AC/DC module). Only the law of electrical conduction introduces the dependence on the material, through the way in which the electrical conductivity affects the distribution (inside the head) of the induced current density. However, it is very important that the geometry and structure of the head be present for locating the spatial distributions of all electromagnetic quantities.

Another comment concerns the **stimulus characteristics**. The application of the cable theory based on the quantification of the *AF activation function* is less appropriate in TMS than in long-fiber stimulation (spinal cord or peripheral nerves), due to the complex anatomical structure of the cortex; at the same time, the induced current density distribution ($\mathbf{J}_{\text{in}}$) seems to be a better indicator of the stimulus.

Although it is directly related to the coil current (which is the externally controlled quantity in the TMS process), the magnetic field analysis does not provide specific information about the stimulus; the waveform and spatial distribution of the stimulus associated with the induced current density ($\mathbf{J}_{\text{in}}$) depend on the coil current waveform and the applicator configuration (geometry and position), as shown by the correlation of the results in this case study. Thus, it is clear that the maximum values of the stimulus do not occur in the same locations where the induction **B** has maximum values (Figure 3.2) nor when $\mathbf{B}(t)$ reaches its maximum value (0.1 ms, according to Figure 3.3.a).

According to the electromagnetic theory associated with TMS, two categories of time evolutions correspond to the quantities involved: $\mathbf{B}(t)$ and $\mathbf{A}(t)$ have waveforms similar to the inductor current $i(t)$, while $\mathbf{E}_{\text{in}}(t)$ și $\mathbf{J}_{\text{in}}(t)$ and Jint depend on the temporal variation rate of the same current (i.e. the time derivative of the current $\mathrm{d}i/\mathrm{d}t$)). This derivative is maximum at the origin of the current pulse, therefore the stimulation is effective in the first moments of its triggering, i.e. immediately at the beginning of the TMS process. This indicates the observation that the maximum values of $\mathbf{J}_{\text{in}}$ and $\mathbf{B}$ are not simultaneous (see the waveforms in Figure 3.3) and that the stimulation is most effective in the first moments of the current pulse ($t < 0.1$ ms). For this reason, $t = 5$ µs was the time selected to display the results in Figure 3.2, considered relevant for effective stimulation.

In this analysis, the transient regime was simulated over a time interval corresponding to an entire pulse (1 ms), but the results clearly show that only the beginning of the pulse, the first microseconds, is relevant for TMS. In order to pursue other objectives in the continuation of this study, the possibility of minimizing the duration of the simulated time interval will be evaluated, as well as a possible equivalence of the first moments of the pulse with a fragment of a sine wave, which would allow replacing the transient regime with a harmonic regime, much more advantageous and economical in terms of numerical analysis and simulation.

Regarding the nominal **values of the electrical and magnetic quantities involved in TMS**, the following is noted. The applicator coil and the conductive tissue inside the head are inductively coupled, with the specification that the induced current density in the head is several orders of magnitude (5 – 6) lower than the current density through the inductor coil. Typically, induced electric fields with intensities above 100 V/m are considered effective for nerve stimulation (Ueno & Sekino, 2016; Roth, 1994), which roughly corresponds to current densities above 10 A/m² in the brain.

Regarding magnetic induction, the inductor coil, operating at a particularly high current (kA), produces a magnetic field of maximum intensity (typical values of 2 – 3 T) near its inner surface, while for the head area the maximum values (of 0.5 – 2 T) are reached on the coil axis (the values decrease with distance and the maximum ones are right in the center of the coil).

Through the numerical analysis performed, objectives were pursued to confirm the validity of the model and the opportunity for its further use, for more varied application analyses:

- Model behavior in accordance with the electromagnetic field theory applied in TMS
- Spatial localization of phenomena - identification of the correspondence between the applicator positioning and the spatial distribution of electromagnetic quantities: magnetic induction and induced current density
- Synchronization of phenomena - identification of the correspondence between the time variation mode (waveform) of the inductor current (respectively of the magnetic induction) and the waveform of the induced current density, respectively of the stimulus
- Finding correspondences between the controllable characteristics of the *input quantities* in the TMS process and respectively the efficiency of the *output quantities* (useful); we identified that:
    - *input quantities*: current through the applicator (characterized by waveform and amplitude) and applicator configuration (shape and positioning relative to the head),
    - *output quantities*: induced electric field intensity, induced current density (important by size and moment of maximum stimulation efficiency).

Correlations of this type are very useful in TMS therapy, but in general the practice is based on the therapist's specialist experience and on empirical approaches, through successive trials with parameter adjustment. Simplified modeling is not so precise to provide directly applicable clinical solutions, but it can contribute to the education of the practitioner, to the formation of a better perception of biophysical and medical effects. It is also particularly useful in design, either in the evaluation of new equipment (especially applicators), or in the optimization of equipment and electromagnetic input quantities.

In contemporary times, the development of neuromodulation techniques is conditioned by: the evolution of medical expertise (through the number of practitioners and their skills) and the access of patients to specialized centers, the development of therapeutic technologies (devices and protocols) and their integration into current medical practice (including coverage by health insurance).

Engineering will continuously support the development of this field by designing and manufacturing devices (more efficient, biocompatible, easy to use, cheap and accessible), by explaining physical phenomena and processes, as well as the complex interactions between physiology, anatomical tissues and electromagnetic fields.

In the case of TMS, for example, the distribution of the induced electric field and the localization of the stimulus are essential aspects, and measurements cannot determine this type of data. The analysis presented here highlights the medical utility of theoretical principles, practical approaches specific to electrical engineering, as well as current technical methods and skills. Some phenomena of subtle interaction between electromagnetic and biophysical processes could be addressed by numerical simulation, which benefits from a collection of specific methodologies and tools developed and mastered by engineers.

The progress of non-invasive neuromodulation techniques is inconceivable without the control of the distribution of the induced electric field and effective stimuli inside the human body, which is possible only through precise simulation; in vivo measurements are practically excluded. Numerical models could be successfully used for the development of TMS strategies and therapeutic protocols, becoming valuable tools for the optimization of equipment (especially applicators). The use of simulation and the improvement of the accuracy of the models (through detailed anatomical structures and realistic dielectric properties) would also contribute to obtaining more precise explanations and a deeper understanding of the neuromodulation phenomena.

4 Analysis by current waveform, in frequency domain vs time domain

4.1 Comparative analysis in the time domain and frequency domain, respectively, on 2D and 3D numerical models

In the simulation of TMS phenomena, a comparison is made in terms of efficiency and accuracy between two different numerical approaches based on the regime applied for the time variation of electromagnetic quantities:

(*) *numerical analysis in the time domain* – is based on the modeling of the inductor current in the form of a monophasic pulse and a transient regime (variable in time) is studied step-by-step;

(**) *numerical analysis in the frequency domain* – the inductor current is considered with harmonic variation in time, and the modeling of the harmonic regime of electromagnetic quantities is approached through complex representation.

In all other aspects (geometry and dimensions of the computational domain, material properties, boundary conditions, density of the discretization network) the models being compared are identical.

The objective is to quantitatively demonstrate that frequency domain analysis can successfully replace time domain analysis with considerable savings in computational resources for simulating the short interval of rapid increase in the amplitude of the applied stimulus, an interval in which the TMS procedure is actually effective.

For practical reasons, to simplify the expression, acronyms are defined in the diagram presented in Table 4.1 for the models that will be worked with further; for precise identification, several essential characteristics are specified for each model, the shape and structure of the head are represented.

Table 4.1 Summary of the main features of the compared models

Acronym	Model description (xD, inductor current, regime, analysis type)	Head models with inhomogeneous structure
3D-TIMP	**Inhomogeneous 3D model** **Pulse inductor current** $$i(t) = \frac{U_0}{L}\, t\, e^{-\propto t}$$ $t_m = 0{,}1$ ms; $\mathrm{d}I/\mathrm{d}t = 2{,}18 \cdot 10^8$ A/s Transient quasi-steady state Time domain analysis	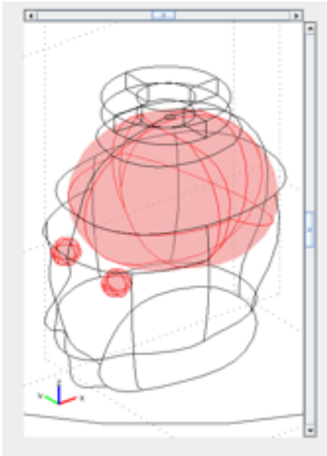 Figure 4.1 Inhomogeneous 3D model, built on the shape of the SAM head
3D-FRECV	**Inhomogeneous 3D model** **Sinusoidal inductor current** $$i(t) = I_m \sin 2\pi f t$$ $$I_m = 8 \text{ kA}; \ f = 4{,}35 \text{ kHz}$$ $t_m = 0{,}057$ ms; $\mathrm{d}I/\mathrm{d}t = 2{,}18 \cdot 10^8$ A/s Harmonic quasi-steady state Frequency domain analysis	
2D-TIMP	**Inhomogeneous 2D model** **Pulse inductor current** $$i(t) = \frac{U_0}{L}\, t\, e^{-\propto t}$$ $t_m = 0{,}1$ ms; $\mathrm{d}I/\mathrm{d}t = 2{,}18 \cdot 10^8$ A/s Transient quasi-steady state Time domain analysis	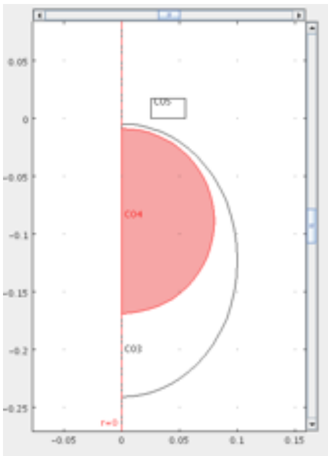 Figure 4.2 Inhomogeneous 2D model based on axial symmetry and made up of simple geometric figures
2D-FRECV	**Inhomogeneous 2D model** **Sinusoidal inductor current** $$i(t) = I_m \sin 2\pi f t$$ $$I_m = 8 \text{ kA}; \ f = 4{,}35 \text{ kHz}$$ $t_m = 0{,}057$ ms; $\mathrm{d}I/\mathrm{d}t = 2{,}18 \cdot 10^8$ A/s Harmonic quasi-steady state Frequency domain analysis	

4.2 Results

The comparison between the simulation results is further made for models in the presented categories, on distributions of the inductive magnetic field (spectra and graphs), as well as on maximum values of the induced current density in the head area.

Inductive magnetic field analysis – 3D models compared to 2D

Figure 4.3 highlights a comparison of results regarding the magnetic induction field in models built with 3D versus 2D geometry. The main characteristics of the distribution of magnetic induction in space are similarly highlighted (orientation of field lines around current-carrying conductors, spectrum symmetry), and the range of values distributed in the cross-sectional plane of the representation is practically the same, as can be seen both in the color spectra and in the distributions on the observation lines.

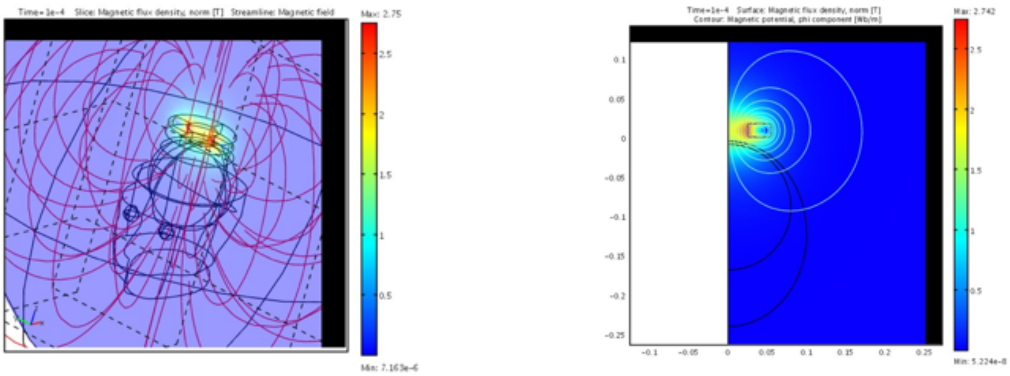

a) Color map of magnetic induction and spectrum of magnetic field lines

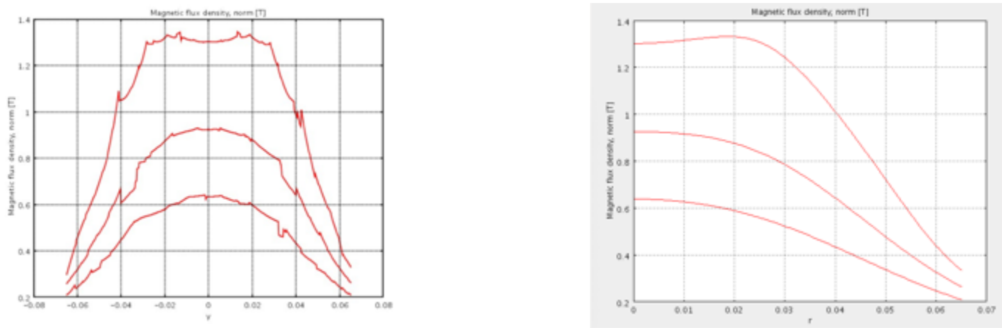

b) Distributions of magnetic induction along horizontal observation lines, included in the frontal section plane through the head, at elevations *z* = -0,01m; -0,02m; -0,03m measured starting from the base of the inductor coil (elevation *z* = 0) (the curves show decreasing levels of values with increasing elevation *z*)

Figure 4.3 Magnetic field distributions (magnetism vector magnitude at peak values) obtained for equivalent 3D (left) versus 2D (right) models; 3D-TIMP vs. 3D-FRECV, respectively 2D-TIMP vs. 2D-FRECV, are not shown separately here for comparison, because the results are practically identical.

Figure 4.3.a shows the comparative (for 3D/2D) color maps of magnetic induction together with spectra of magnetic field lines, at moments of maximum values – for the

equivalent models it is the pulse peak (3D-TIMP and 2D-TIMP models), respectively the maximum of the sinusoid (3D-FRECV and 2D-FRECV models); in both cases the current has the maximum value of 8 kA. The graphs in Figure 4.3.b show variations of magnetic induction along observation lines included in the frontal plane (cross-sectional) and parallel to the plane of the inductor coil (z = 0), at three distances from the coil, i.e. at the elevations: z = -0,01m; -0,02 m; -0,03 m; the value levels naturally decrease with increasing distance from the coil.

It is important to mention that the results obtained in the time domain and in the frequency domain for the magnetic field inductor are identical in the cases of 3D-TIMP with 3D-FRECV and 2D-TIMP with 2D-FRECV, respectively. Regarding the magnetic field, the two categories of *equivalent models* (frequency analysis versus time analysis) give identical results as long as the evaluation is made at the same value of the inductor current (I_m = 8 kA in this case). Due to the identity of the values, it was considered that it was not necessary to present the results from both categories of models here.

In the data in Figure 4.3, a very good approximation between the magnetic field distributions simulated with the 3D models (left) versus the 2D ones (right) is also noted. From this it can be concluded that for the evaluation of the inductive magnetic field, if the symmetry of the model allows it, the 2D calculation provides an optimal working solution - that is, results of good accuracy are obtained at a reduced consumption of computing resources.

Induced current density analysis

Another category of illustrative results for the comparison between the models described here refers to the quantity that quantifies the efficiency of stimulation through the TMS procedure – *the induced current density* calculated as the modulus of the vector $|\mathbf{J_{in}}|$.

For 2D models

These quantities were calculated for the 2D models, and the results are presented in Figure 4.4 for the maximum values of the quantity $|\mathbf{J_{in}}|$, respectively:

a) *for the pulse* (transient regime, time domain analysis - 2D-TIMP model) – results are collected at the time instant timp $t = 2\cdot10^{-6}$ s (i.e. at the beginning of the inductor current pulse), because the rate of increase in time of the current (waveform slope) and respectively of the magnetic induction is the highest, therefore maximum values of the electric field and of the induced current density are obtained;

b) *for the sinusoid* (harmonic regime, frequency domain analysis - 2D-FRECV model) – the maximum values of the quantity |Jin| are taken as the calculation result, offered as a solution to the complex calculation.

The quantity represented in the graphs is the modulus of the induced current density $|\mathbf{J_{in}}|$; for 2D models based on axial symmetry, the vector $\mathbf{J_{in}}$ has only a component perpendicular to the calculation plane (azimuthal component). In the case of frequency analysis, the results provided by the calculation program are complex numbers; thus, the calculation of the modulus $|\mathbf{J_{in}}|$ is done as for a complex number (the square root of the sum of the squares of the real and imaginary parts).

To facilitate comparison with the results of the 2D models, values of magnetic induction and induced current density were collected along the same three observation lines included in the frontal plane through the head and drawn horizontally, parallel to the plane of the inductor coil, at three distances from the base plane of the coil, i.e. at the elevations: z = -0.01m; -0.02 m; -0.03 m (the base of the coil is at elevation z = 0). To identify the graphs, the general rule is taken into account that the levels of values naturally decrease with increasing distance z from the coil, and the sudden decrease in amplitude occurs at the transition between the brain and skull subdomains.

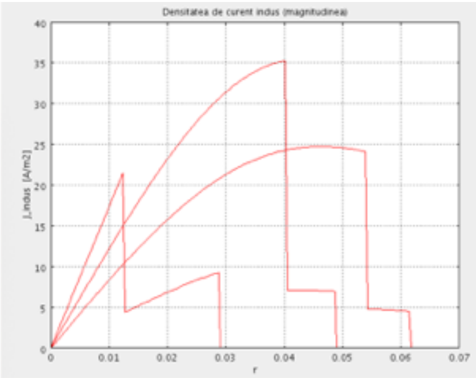

a) Case of analysis on the current pulse at t=2·10^{-6} s s (2D-TIMP model)

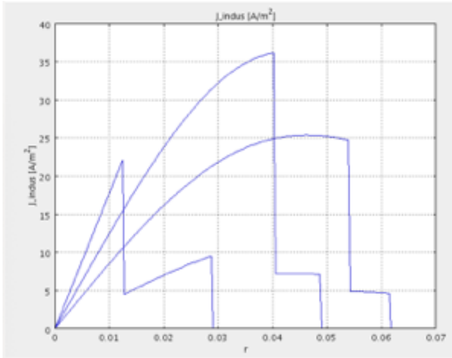

b) Case of analysis on sinusoidal current at maximum values (2D-FRECV model)

Figure 4.4 Distributions of the induced current density (modulus of the vector quantity, respectively of the complex number) along horizontal observation lines, included in the frontal section plane through the head, at elevations z = - 0,01m; -0,02m; -0,03m measured starting from the base of the inductor coil (elevation z = 0) (from left to right, the curves are in increasing order of the distance z from the coil;)

The sets of three curves are distributions of the quantity $|\mathbf{J}_{in}|$ according to the radial coordinate (in cylindrical coordinate system for 2D models), at three elevations (z = - 0.01 m; -0.02 m; -0.03 m) measured starting from the base of the inductor coil (elevation z = 0). The three curves correspond in order, from left to right, to the increasing values of the z distances from the coil, and the sudden decrease in amplitude occurs when passing between the brain and skull subdomains. As the comparison in Figure 4.4 for equivalent 2D models shows, the two ways of approaching the problem (in time / in frequency) lead to similar results – spatial distributions of the same type, very close in values; practically, the errors expressed as relative differences are below 5%.

For 3D models

The electromagnetic field analysis problem in the TMS simulation was solved in a similar way with the 3D model to compare the two numerical analysis modes. The results are presented in the form of magnetic induction and induced current density distributions (at the moment of reaching the peak values of the latter), in Figure 4.5 for *the time domain analysis* (pulse waveform) and in Figure 4.6 for the *frequency domain analysis* (harmonic waveform), respectively. For the time domain analysis, the moment t = 2·10^{-6} s was chosen in the representation, very close to the triggering of the inductor current pulse, respectively at the maximum of the induced current density. The same condition of maximum induction effect was imposed in the collection of the frequency domain analysis results.

In the case of the induced current density, the results of the 3D models are also very close to those provided by the 2D models. For the *time domain analysis* (transient regime for the pulse waveform) the graphs presented in Figure 4.5.b are compared with those in Figure 4.4.a, preserving both the distribution trends (the spatial distribution is dependent on the applicator configuration) and the range of values (comparable orders of magnitude are obtained).

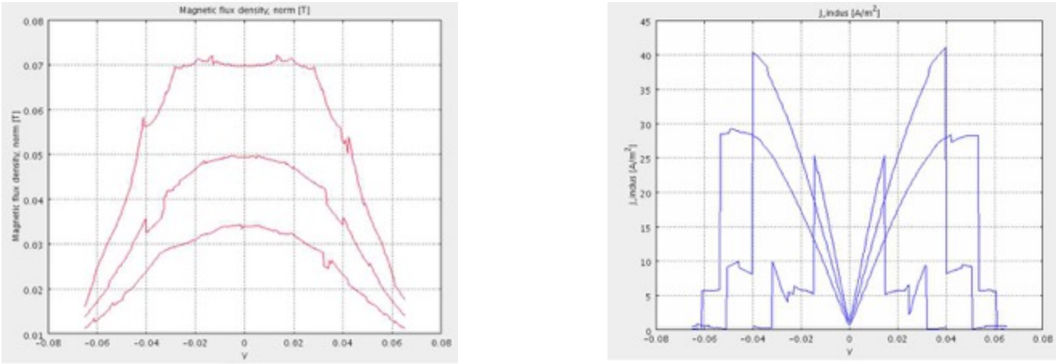

a) Magnetic induction |**B**| b) Induced current density |$\mathbf{J}_{in}$|

Figure 4.5 Results obtained with the 3D-TIMP model for *the time domain analysis* of the electromagnetic field associated with the TMS procedure; values are extracted for the moment $t = 2 \cdot 10^{-6}$ s, following horizontal observation lines (drawn through the head in the frontal section plane), at elevations z = -0,01m; -0,02m; -0,03m measured starting from the base of the inductor coil (z = 0) (the | $\mathbf{J}_{in}$ | graphs are compared with those obtained on the 2D models – Figure 4.4.a)

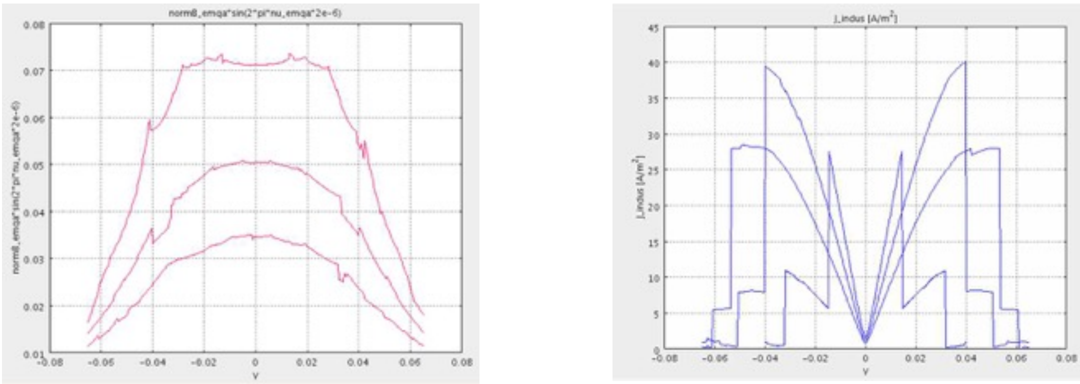

a) Magnetic induction |**B**| b) Induced current density |$\mathbf{J}_{in}$|

Figure 4.6 Results obtained with the 3D-FRECV model for the *frequency domain analysis* of the electromagnetic field associated with the TMS procedure; values are extracted for the moment $t = 2 \cdot 10^{-6}$ s, following horizontal observation lines (drawn through the head in the frontal section plane), at elevations z = -0,01m; -0,02m; -0,03m measured starting from the base of the inductor coil (z = 0) (the graphs are compared with those obtained on the 2D models – Figure 4.4.b)

The same type of results were generated for the *frequency domain analysis* (harmonic waveform) with the 3D-FRECV model, Figure 4.6, with distributions extracted for the magnetic induction and for the induced current density, under similar conditions (same electromagnetic quantities - for the same moments of time in the case of induction and at maximums of the induced current density). If we compare the graphs for the induced current density presented under similar conditions - in Figure 4.6.b from the 3D-FRECV model with those in Figure 4.4.b from the 2D-FRECV model, a high degree of similarity is observed.

Regarding the magnetic induction, it is observed, as in the case of the 2D models, that the time and frequency analysis give practically identical results, the evaluations being made at the same values of the current through the inductor coils.

4.3 Comments and conclusions

In this study, numerical models for electromagnetic field analysis were defined for simulating the TMS procedure, covering the analysis regimes in the time domain and in the frequency domain, respectively, aiming to evaluate the option of replacing the transient regime study for a pulse-shaped inductor current with a sinusoidal current (the frequency is chosen from certain equivalence considerations exposed and demonstrated in the thesis). For each regime, both a 3D model of the inhomogeneous head built on the SAM mannequin and an idealized 2D model were used, based on simulating the head with simple geometric shapes (ellipsoid and spheres) and applying axial symmetry. Studies carried out on various geometric models are present in the literature and the criteria for choosing one type of working model or another were sought, depending on the objectives of each study and the accessible computing resources.

Frequency domain analysis can replace *time domain analysis* for determining and locating significant electromagnetic quantities in TMS, if the frequency of the harmonic wave is determined correctly (i.e. based on the equivalence of the slope at the origin of the sinusoid and pulse signals). Solving the problem in the frequency domain (in the quasi-stationary harmonic regime) is incomparably more economical than the time domain approach, in terms of computational resources (memory volume for numerical analysis and solution storage) and in terms of solution duration. Here, however, it can be noted that the time domain analysis is performed for a specified duration, which in the case of TMS can be reduced to the first moments of the pulse (the interesting operating point in TMS is where the slope of the inductor signal is maximum); however, for a correct calculation (derivatives and integrals in time), it is necessary to solve several time steps, compared to a single calculation step, in frequency analysis. The thesis provides quantitative data on resource consumption for each individual case.

The correct equivalence of the results between the two types of analysis described is based on special attention paid to the significance of the electromagnetic quantities in each of the two working modes (quasi-stationary harmonic versus quasi-stationary transient); thus, one can operate with instantaneous quantities / time-averaged quantities on a harmonic waveform, effective quantities / maximum quantities (modulus), vector components / vector modulus, etc.

5 Simplifications in the description of models to reduce computational effort

5.1 Simplified representations for the applicator

5.1.1 Introduction, objective and approaches from the specialized literature

The present study evaluates the impact of the coil representation method on the electromagnetic field simulation results performed in Comsol Multiphysics. *The objective* is to optimize the applicator representation so that the savings in computational resources are balanced in relation to the accuracy of the magnetic field simulation produced. Three distinct coil models are compared in order to identify the most efficient representation, which offers the lowest possible consumption of computational resources, while maintaining a convenient level of accuracy of the results. In order to make a more objective comparison between the three coil representations chosen in this study, a model was built that includes all the geometry elements necessary to describe each of them:

(1) *N* turns formed by profiled conductor, separated by conductor insulation and each turn having a given realistic current density;

(2) A massive conductor with the cross-sectional area determined as the equivalent area of the coil section, on which the $N{\cdot}i$ solenoid is applied; the model was used in previous chapters and is presented in subchapter 3.2.3 *Magnetic field source*, together with the calculation method of the equivalent current density through the solid section of the coil;

(3) *N* filiform conductors positioned on the average fiber of the real conductors (in the center of the profiled conductors); filiform conductors in 2D models are introduced as point elements to which a realistic value *i* of the current intensity is assigned.

The coil with its real structure is represented in section in Figure 5.3.a, with the corresponding geometric data, and the three modes of representation in the model, listed above, can be identified in Figure 5.3.b; the transition from one model to another is made by assigning different data (material properties and magnetic field sources - currents / current densities). A triangular element mesh, automatically generated with the *Extra Fine* density type (selected in Comsol for automatic generation) was used to discretize the computational domain; in addition, for the domains that form the head, the restriction for the maximum size of the mesh elements was imposed at 0,5 mm, according to the image in Figure 5.3.c. This discretization method adapts the mesh to the geometric details and to the type of problem (type of differential equations involved), ensuring a convenient density also in the computational area of the quantities of interest (current density induced in the head area). The presence in the computational domain of all geometry elements (for the three coil models) constrains the network and ensures that its structure and density remain the same for good comparison of results.

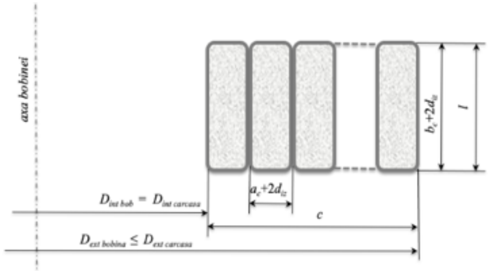

a) Schematic representation of the TMS coil with dimensional details
($D_{int\ bob}$=50 mm; $D_{ext\ bob}$=111,6 mm; l=15,4 mm; c=30,8 mm; a_c=1,8 mm; b_c=15 mm; d_{iz}=0,2 mm)

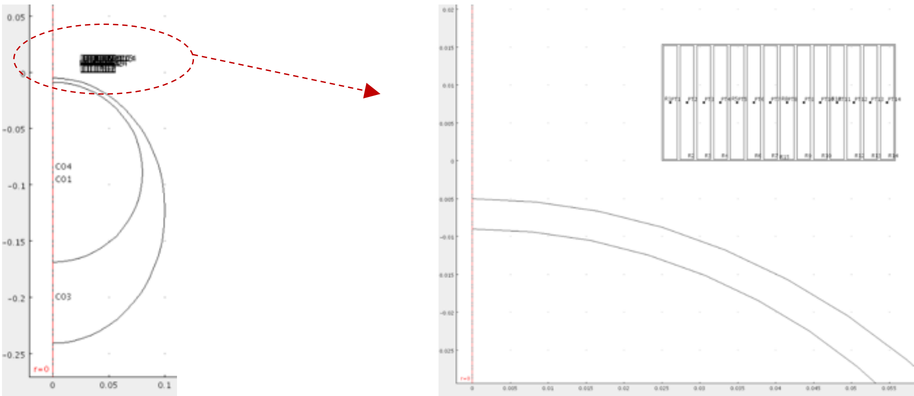

b) Geometry represented in Comsol Multiphysics (entire domain – left and coil detail – right) with the possibility of describing any of the three representation models defined above, only through the data entry mode

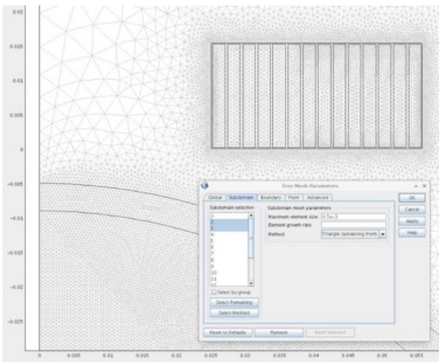

a) c) Discretization in Comsol Multiphysics for the model that includes the geometry details for all three cases, ensuring that the same mesh configuration is maintained

b) (Extra Fine mesh and mesh refinement in the head area)

Figure 5.1 Representation of the coil with the coverage of the three models

The way of describing the magnetic field sources (attribution of current density or current intensity) is suggested in Figure 5.4; the current densities for the massive conductors present in models (1) and (2) are marked, respectively the current intensity assigned pointwise in model (3). For comparison, the magnetic field lines are also drawn in each case.

Model (1)

Realistically represented coil - *N* turns insulated from each other; the realistic current density is assigned to the conductor cross-section surface of each turn

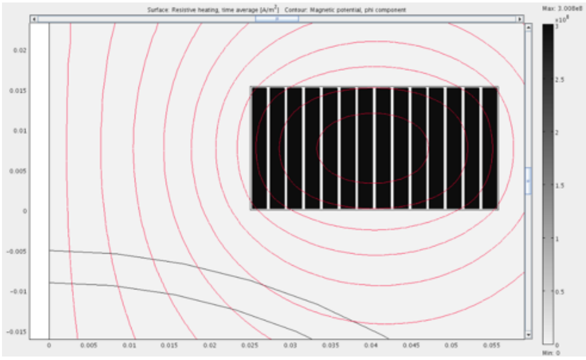

Model (2)

The coil represented as a single equivalent solid conductor – the equivalent current density is assigned to the entire section through the coil (conductor and insulation)

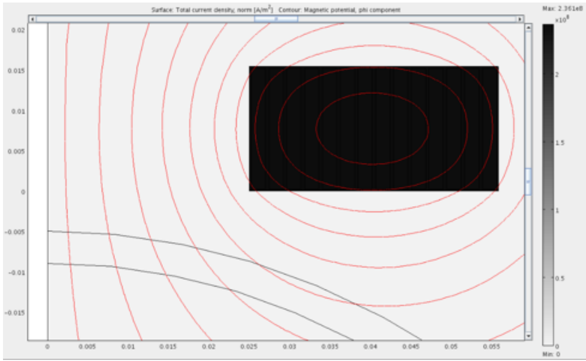

Model (3)

The coil represented with a filiform conductor (on the average fiber of the real coil) – the current value is assigned pointwise to the geometric center of each turn

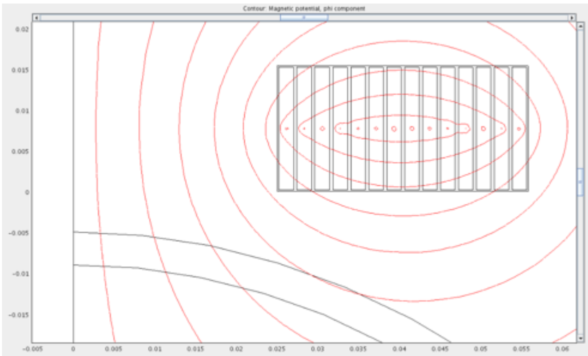

Figure 5.2 The coil representation models in the three cases and the magnetic field spectra

5.1.2 Results and post-processing

The results are presented in Figure 5.3 in the form of color maps of magnetic induction and the spectrum of magnetic field lines; it is observed that in the area of interest (i.e. in the head area) the distributions and values of induction are comparable for the three ways of representing the coil winding.

Model (1)

Realistically represented coil - *N* turns insulated from each other

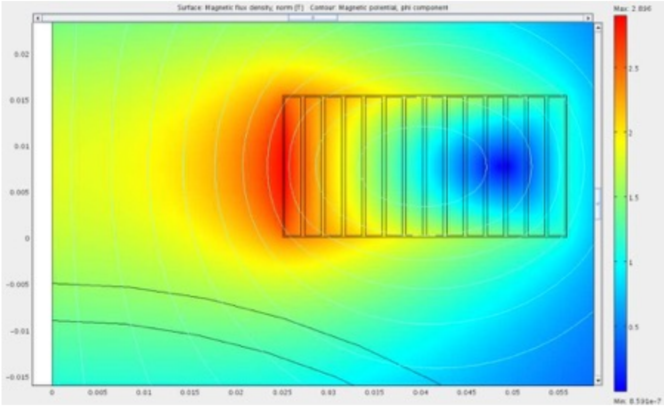

Model (2)

The coil represented as a single solid conductor with equivalent current density

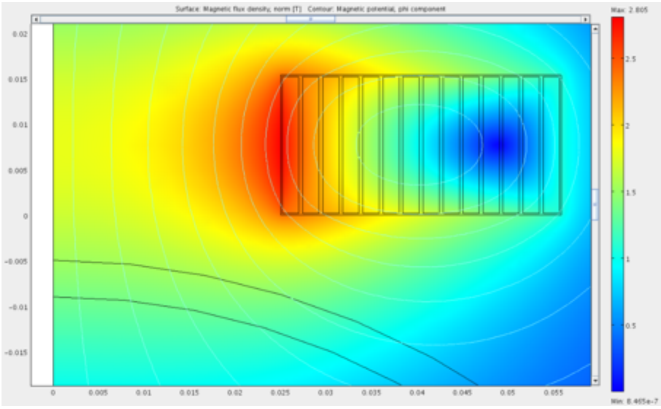

Model (3)

The coil shown with a filiform conductor (on the middle fiber of the real coil); in the image the range of values for B is limited to max. 3T to avoid extremely high point values near the filiform conductors

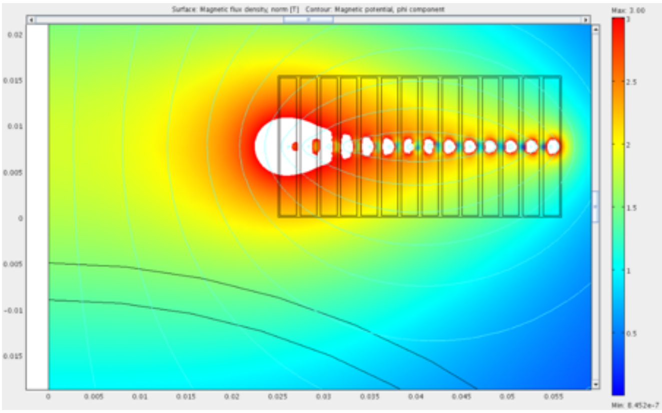

Figure 5.3 Color map of magnetic induction and magnetic field lines corresponding to each of the three circular coil representation models; in all cases, the complete geometry and the same discretization network are used, and the differences between the models are obtained from data adaptation (results are for the maximum coil current I_{max} = 8 kA)

A better comparison between the three models is given by Figure 5.4, where the distributions of the magnetic induction and the induced current density are represented, along horizontal directions (included in the frontal plane of the head) at two elevations on the z axis (two distances measured from the base of the coil to the head). In both sets of results, the values obtained for the three coil models are very close. If we consider that the first model offers the most accurate representation and is taken as a reference (green curves), we observe that very slightly lower inductions result in the representation of the coil by a massive, homogeneous coil, equivalent to the real coil in terms of overall dimensions and having an equivalent current density (blue curves), as well as in the representation of the coil with filiform conductors (red curves). It should be noted that in all cases the variable field effects in massive conductors are neglected, by neglecting the electrical conductivity of the material.

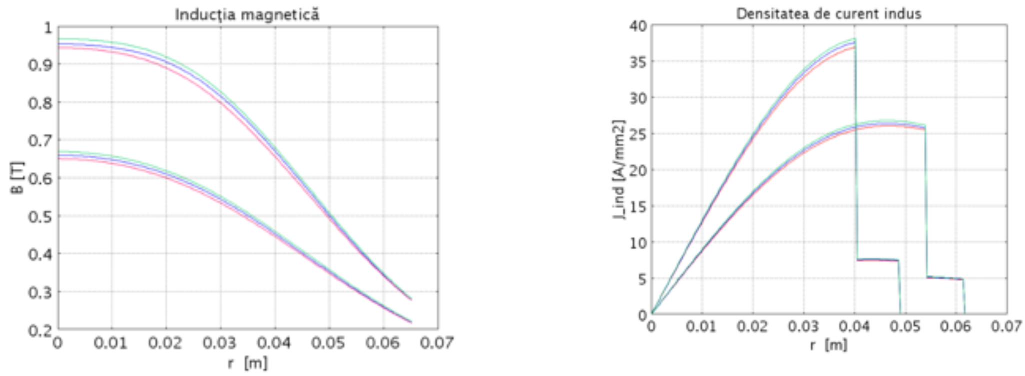

a. Magnetic induction b. Induced current density (absolute value)

Figure 5.4 Distribution of magnetic induction and induced current density along two horizontal observation lines, drawn through the head region, at elevations *z* = -0,02 m (higher values) and -0,03 m, respectively; model (1) – green, model (2) – blue and model 3 – red

5.1.3 Comments and conclusions

The study shows that the need for a detailed representation of the coil is not justified; this involves geometric details and a very fine discretization network. It is important to respect two elements of the description of the magnetic field source: the magnitude of the solenoid and its spatial distribution as close to reality as possible. The law of the magnetic circuit makes the connection between the source current (the value of *I*) and the magnetic induction it produces, depending on the distance between the source current and the calculation point. Thus, regardless of whether the source current is distributed over a conductor surface or is concentrated on a wire, or distributed over overlapping turns, it is very important on the induction produced, especially at a distance. The magnetic field is affected in the immediate vicinity of the sources (the conductive areas traversed by the current), but at a short distance the distributions are already similar. What is important is that the value of the source current *I* and the position in space of the conductors are respected. The representation of filiform conductors or that of the equivalent coil bring advantages in reducing the modeling effort and computational resources, without significantly diminishing the accuracy of the solution in the area of interest. This conclusion is especially valuable for 3D models, where the management of computational resources is critical.

5.2 Simplified representations for the head

5.2.1 Introduction, objective and approaches from the specialized literature

The present study aims to evaluate the impact of the head representation method and the degree of detail of the anatomical structure - the component tissues in TMS simulations to analyze the distribution of the induced current density $\mathbf{J_{in}}$ in different areas of the head. The study is done in *harmonic mode*, for cases that allow comparisons with the 3D head model, respectively 2D by *simplifying the number of layers represented* (e.g. a single equivalent tissue type for the entire head or by *representing several layers* of component tissues of the head - skin, adipose tissue, muscle, neuronal tissue, etc.).

The objective pursued aims to evaluate the possibilities of optimizing the representation of the human head in simulations performed in COMSOL Multiphysics so that the savings in computational resources (simplified representation of anatomical structures) are balanced in relation to the accuracy of the results obtained for the distribution of $\mathbf{J_{in}}$.

5.2.2 Simplified geometric patterns for the head

For this case study, the 2D inhomogeneous model based on axial symmetry (in cylindrical coordinates *r, z*) and consisting of simple geometric figures will be used to represent the head. In a first stage of this study, a comparison will be made between case (a) in which the model is homogeneous in terms of material properties (σ_{brain} throughout the head) and case (b) in which the model is layered with 2 biological tissues with different electrical properties (σ_{bone} and σ_{brain}). In a next stage of the study, a comparison will also be made with case (c) in which the model is layered and has 5 biological tissues with different electrical properties (σ_{skin}, σ_{bone}, σ_{LCR} , $\sigma_{s\ white}$ and $\sigma_{s\ grey}$ - in order from the outside of the head model to the inside).

5.2.3 Results and post-processing

The numerical analysis was performed applying data, hypotheses, FEM implementation method already described and applied for the 2D models operated with in Chapter 4, when considering the inductor current with harmonic variation in time. Figure 5.9 presents by comparison the distributions of the induced current density (J_{ind}) for the two 2D models described previously.

In the homogeneous case (a), a maximum intensity of the induced current density of approximately $48{,}16\ \mathrm{A/m^2}$, is observed, with a smoother distribution gradient, diffuse throughout the depth of the hemisphere, with a maximum location at the upper interface of the head, close to the coil. The two-layer model (b) presents a lower maximum value, of $39{,}87\ \mathrm{A/m^2}$, located in the brain subdomain, explainable both by the higher electrical conductivity value of the “brain” environment compared to the “skull”, and by the greater distance of the area of localization of the maximum values from the inductor (coil). A clear transition zone is observed between the two layers – the current is attenuated in the deep area (brain). This difference is explained by the presence of the outer layer with lower conductivity, which limits the penetration of the current towards the internal region (brain), thus demonstrating that the presence of the cranial bone influences both the amplitude and the localization of the induced current in the electromagnetic simulations.

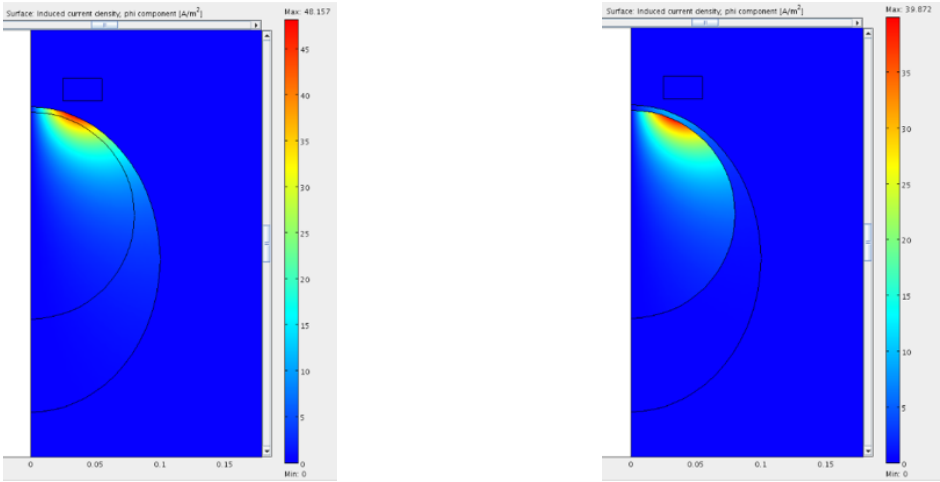

a) The homogeneous model in terms of material properties (skull and brain have the same electrical properties)

b) The layered model, inhomogeneous in terms of material properties with 2 layers (skull and brain with distinct properties)

Figure 5.5 Comparison between the results of the 2D models for the calculation of the induced current density (J_{ind}) (the color spectra show maximum values in the 2 head representation models (a) and (b) Note: The (J_{ind}) values are the same as those given by Comsol Multiphysics for the “Induced current density” quantity; here the modulus was chosen, i.e. *abs(Jiphi_emqa)*.

5.2.4 Comments and conclusions

The representation of the head by a layered structure is a rough anatomical approximation. However, it is frequently used in the literature for qualitative evaluations or, as proposed by the present studies, to quickly and economically test, under similar conditions, different constructive variants of the equipment, specifically of the TMS applicator.

The results obtained show notable differences between the two models, both in terms of the maximum values of the induced current density and its spatial distribution. The homogeneous model tends to overestimate the current level in the cerebral region and the distribution of values is exclusively influenced by the distance from the inductor, not taking into account the attenuation effect due to the cranial bone. The introduction of an additional layer with lower conductivity (σ_{bone}) leads to a clear reduction of the induced current intensity and to a more realistic localization of it. These findings support the need to use layered models, which include at least the main components of the cranial structure. In a future stage of this study, the case where the model is represented in even more detail by extending it to 3-5 biological layers/tissues (including skin, adipose tissue, bone, CSF, brain) will be compared, to ensure a more realistic and robust simulation of bioelectromagnetic phenomena.

6 Analysis of some side effects of the TMS procedure

6.1 Human exposure (patient and operator) to the induced magnetic field

The research program has as an essential component the analysis of the electromagnetic field under specific TMS conditions. The major contraindications for the application of TMS-type procedures aim to avoid electromagnetic interference between the very strong inductor field (up to 2 – 3 T in the immediate vicinity of the applicator and respectively values of 0,5 – 1 T at distances of 10 – 15 cm from the applicator) in an area where there may be metallic objects (dental prostheses, metallic implants in the face or head area), active implants (auditory, neurological), or other therapy or communications equipment, as well as parts of the therapist's body.

6.1.1 Regulations on human exposure to low-frequency magnetic fields

Human exposure to electromagnetic fields is currently regulated by international normative documents; the best known are: the ICNIRP recommendations for the low and medium frequency range (ICNIRP, 2010) and which apply in Europe, respectively the IEEE C95.1 standard (IEEE, 2019) for the American continent. The provisions of these documents aim to limit the levels of human exposure to electromagnetic fields, in order to minimize the risk of health damage; there are different regulations for the general public (unintentional and uncontrolled exposure, regardless of age, gender, health status, incidence of exposure conditions, etc.) and for professionals working in environments with assumed and controlled exposure.

6.1.2 Magnetic field exposure for subjects/patients

Individual TMS or rTMS sessions do not pose the risk of significant exposure to the magnetic field, since the total time is short. Numerous research studies in neurology and psychiatry have been published, such as (Loo, 2008), or (Di Lazzaro, 2009), which indicate typical protocols for different pathologies, applied for relatively long periods and in which, in addition to the targeted clinical effects, side effects, such as those caused by prolonged and repeated exposure to variable magnetic fields, were monitored. In all these cases, no adverse effects due to human exposure to electromagnetic fields were recorded.

In conclusion, exposure to variable magnetic fields through TMS is considered a safe procedure for most patients, if safety protocols and subject selection criteria are rigorously followed. The method's efficiency, lack of pain, and ability to provide relevant neurophysiological information support its clinical use, while risks can be significantly diminished by individualized adaptation of stimulus intensity and careful monitoring of the patient's response.

6.1.3 Magnetic field exposure for therapists

Safety issues are rarely addressed for operators who are exposed to variable magnetic fields for several hours each day for years by performing TMS. Guidelines on occupational exposure levels to electromagnetic fields have been proposed by the International Commission on Radiation Protection (ICNIRP, 2010) and by a directive of the European Parliament (Directive 2004/40/EC (Riches, 2007a), eventually adopted as Directive 2013/35/EC on the protection of workers from occupational exposure to electromagnetic fields). This directive introduced exposure limit values for workers as well as action values (magnitude of the magnetic field that is directly measurable). However, long-term effects are not included in the scope of the directive. In its original form, from 2004, this directive was to enter into force on 30 April 2008 in all EU countries, but transposition was delayed by resistance from those responsible for operating nuclear magnetic resonance imaging equipment, where the imposed provisions could not be met. Occupational exposure to magnetic fields has been measured for MRI units (Riches, 2007a). Exposure values are 100 times below the recommended exposure limits (Bradley, 2007), except in the case of interventional procedures (Hilli, 2005; Riches, 2007b). Regarding TMS/rTMS, a study was conducted using the MagPro device (Medtronic), the MC-B70 coil (figure 8), at a frequency of 5 Hz and a stimulus intensity of 60–80% of the stimulator power (Karlström, 2006). Under these conditions, it was found that the exposure of workers up to distances of approximately 0,7 m from the coil surface exceeds the accepted limits for occupational exposure. TMS equipment may include a fixed positioning support for the applicator (articulated arm), useful in longer therapeutic sessions, allowing medical personnel to stand at a greater distance from the magnetic field source.

6.1.4 Induced electric field, induced electromotive forces

The strong and rapidly increasing pulse of the magnetic field emitted by the TMS coil can induce electric fields and therefore high electrical voltages in electrical conductors and electronic devices near the applicator. Sometimes, in the clinical environment, the TMS procedure is applied successively with EEG recordings (the electroencephalogram is obtained with recording electrodes fixed to the scalp); even if the interventions are not carried out simultaneously and the EEG circuits are not in operation, keeping the electrodes connected to the measuring device on the scalp (even if it is turned off) means the presence of electrical circuits (conductive wires) in the area of the TMS intervention. The wires that connect to the electrodes used in EEG must be positioned and arranged in such a way that they do not form loops and should be twisted together to minimize the electromotive forces induced in these circuits. If such measures are not taken, the magnetic field produced by the TMS applicator can induce dangerous electromotive forces in the EEG circuits distributed in different regions of the scalp.

6.2 Study of heating effects by analyzing the electro-thermal problem

The heating of the tissues in the head area during a single pulse TMS treatment session (of the induction current) is very small and is estimated to be certainly less than 0,1\ °C (Ruohonen, 2002). It seems that the heating is even lower in areas with significant tissue blood supply (increased perfusion), such as cysts or in cases of stroke (Ruohonen, 2002). The high cerebral blood perfusion provides a safety margin (Brix, 2002). For comparison, the heating in the immediate vicinity of deep brain stimulation electrodes is estimated to be at most 0,8\ °C (Datta, 2006). Eddy currents induced in electrodes and conductive surface implants can cause them to heat up (Roth, 1992; Rotenberg, 2007). The temperature rise depends on the shape, size, orientation, conductivity, and properties of the surrounding tissue of the electrode or implant, as well as the type, position, and stimulation parameters of the TMS coil. Silver and gold electrodes are highly conductive and can become excessively hot, potentially causing skin burns. A temperature of 50°C for 100\ s or 55°C for 10\ s can cause skin burns (Roth, 1992). Radial notching of electrodes and skull plates can also reduce heating by interrupting the path of induced eddy currents. Titanium skull plates tend to have low heating, due to the low conductivity of titanium and the radial notch (Rotenberg, 2007). Brain implants, such as aneurysm clips and stimulation electrodes, can also become hot. Heating brain tissue above 43°C can lead to irreversible damage (Matsumi, 1994).

6.3 Study of the effects of sensory stimulation by producing magnetophosphenes

The application of a relatively high intensity variable magnetic field in the head area can affect excitable sensitive tissues, especially the retina. The typical biological effect when the excitability threshold is exceeded is the triggering of magnetophosphenes, perceived by the subject as luminous visual sensations (sparks, flashes).

Although this phenomenon is not specific to TMS-type procedures (being signaled at extremely low frequencies, usually of the order of tens of Hz), its production is due to the same phenomenon of electromagnetic induction and the appearance of the electric field and the induced current density in the good conductive environment of the retina. The human head model presented and used in the thesis was used for a numerical simulation program dedicated to the dosimetric evaluation of electromagnetic stresses at the eye level, by exposing the head to the uniform magnetic field created by two identical coils in a Helmholtz-type arrangement (Ciocăzanu, 2025 bis). Exposure conditions at the trigger limit of magnetophosphenes were analyzed, with magnetic inductions in the range (20 ... 50) mT and frequencies of 20, 50, 60 and 100 Hz. The study is not detailed in the doctoral thesis, but is seen as a premise for future research in the field of magnetophosphene production.

7 Observational study of a TMS device in the clinical setting

The observation and analysis of the components used in TMS in the clinical environment clarifies issues that are of real use for the numerical modeling analysis performed in the research program. Thus, I took advantage of a good opportunity to have a realistic perception of the equipment used and to see in reality the construction, technical characteristics and operating mode (without a patient in a first stage). At this demonstration of the TMS equipment, I, as the author of the thesis, was kindly received by Mrs. Dr. Cosmina Mureșan, primary care psychiatrist, in her own practice office PSIHIATRIE C&M SRL in the city of Târgu Jiu. I, as the author of the thesis, having a degree in Psychology, obtained in 2023, at the University of Bucharest, asked the doctor to receive me in her office to observe the equipment (construction, parameters and operating technique) and to give me practical information regarding its functioning, operating techniques, protocols used in current medical practice and their efficiency. I was also interested in aspects related to patient feedback and the future of this medical technology in the opinion of the practicing physician.

7.1 Equipment and protocol for applying the TMS procedure

The general setting of the office is shown in Figure 7.1. The office configuration, in addition to the TMS equipment, also includes an adjustable chair with a cushion where the patient will be seated during the treatment.

a) The general framework of the cabinet containing the TMS equipment and the articulated arm for positioning the TMS coil

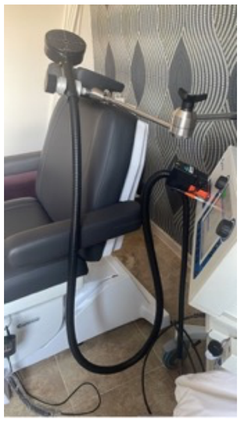

b) Side view with TMS device

Figure 7.1 TMS procedure application cabinet

The device model used is the MagPro R30 produced by the Danish company MagVenture A/S. The device is equipped with the Cool-B65 A/P coil (present in the current study and shown in Figure 7.1) or in other cases the MMC-140 II coil is used, both of which are dedicated to rTMS treatment. The MagPro R30 device is placed on a portable trolley and includes the following main components: the current source for powering the applicator with a front panel that allows setting the current characteristics, the applicator (different models can be mounted to the source circuit) and an applicator positioning system to maintain it in a fixed position. The MagPro R30 is designed for high-precision repetitive magnetic stimulation, being compatible with standardized clinical protocols in depression, obsessive-compulsive disorder and other CE/FDA approved indications. Table 7.1 presents the technical characteristics of the observed TMS device MagPro R30.

Table 7.1 Technical features MagPro R30

Technical features MagPro R30	**Values**
Maximum frequency (pulse sequence)	60 Hz (but 10 Hz is the standard used in depression).
Supply voltage	100–240V, 50/60Hz.
Weight	approx. 26 kg.
Cooling system	active (with water), for Cool coils.
Maintained pulse duration (pulse duration)	adjustable between 20-400 µs.
Touch screen	for parameter control and protocol saving.

Based on the discussion with the therapist about the protocol for applying TMS in treating depression and the information gathered from the specialized literature (Sack, 2023), we completed the protocol described in Table 7.2.

Table 7.2 Steps in a TMS procedure

Stages of the procedure	**Protocol steps**
1. Preparation before the patient arrives	Checking the operation of the MAG PRO R30 device. Checking the cooling system and the integrity of the coil ("figure-of-8" coil for focused treatment). Preparing the patient's file. Ensuring that medical protocols (medical prescription, indication for rTMS) are complete and signed.
2. Receiving the patient	The patient is greeted in a calm and empathetic manner at the reception, given a brief presentation of the session; the patient's identity is verified and the appointment is reviewed. Pre-treatment discussion: discussing any changes in health status since the last session; assessing the existence of any conditions that would contraindicate the session.

3. Setting parameters on MAG PRO R30	Protocol choice for depression: left dorsolateral prefrontal cortex (L-DLPFC) stimulation. Location of the stimulation point: approximately 5 cm anterior to the motor "hot spot". Frequently used parameters: see Table 7.2
4. Patient positioning	The patient is invited to sit in a comfortable armchair with a backrest (see Figure 7.1 TMS procedure application cabinet). The patient's head is secured (adjustable head support or soft fixation system). The head must be stable to prevent movement during stimulation.
5. Coil positioning	Approximately 5 cm anterior to the localized motor point. 45° angle to the midline of the skull. Distance of the coil from the scalp: ideally 0 – 1 cm (the coil can lightly touch the patient's head, without pressing).
6. Determination of motor threshold (at the first session or at reassessments/once a week)	Positioning the coil on the right motor cortex (stimulation for the abductor muscle*short thumb* from the right hand). Increase the intensity until a visible motor response or detectable EMG is obtained in at least 5 out of 10 pulses. Noting the motor threshold and calculating the treatment intensity (maximum intensity of the current pulse through the applicator)
7. Confirmation before stimulation begins	Checking patient comfort. Explaining the expected sensations and asking the patient to report any discomfort.
8. The actual course of treatment	Starting the protocol. Permanent monitoring of patient reactions. Observing any facial spasms and adjusting the coil position if necessary. Periodic discussions to assess patient comfort. Temporarily stop and adjust settings if major discomfort occurs.
9. Ending the session	Closing the protocol on MAG PRO R30. Removing the coil. Post-session discussion regarding the patient experience. Noting any adverse reactions.
10. Feedback and planning	Providing post-session recommendations. Planning the next session (30 consecutive sessions, daily or 5 days/week). Completion of the treatment sheet.

11. Documentation in the medical record	Recording each session in the medical record. Documenting protocol changes. Periodic supervision of equipment calibration.

7.2 Conclusions and directions for future studies

This observational study could be complemented with a next stage that will consist of observing a TMS treatment session of TDM.

Data will be collected through direct observation, completion of the observation sheet, documentary photographs, discussions with the therapist, but also with the patient.

Systematic documentation of the equipment used in rTMS is essential both for evaluating the effectiveness of the intervention and for patient safety. The standardized protocol and careful recording of technical and clinical parameters allow for the replicability of the treatment and the individualized adjustment of future interventions.

Direct observation of the equipment used in rTMS in a real clinical setting has provided valuable insight into how this neuromodulation technology is integrated into psychiatric practice. This experience supports the development of applied research projects that can contribute to improving the equipment, refining treatment protocols and even identifying biomarkers of response.

8 Conclusions

8.1 Obtained results

Within this thesis, studies were carried out with the main aim of streamlining the research process of an engineer who wants to do preliminary research to innovate the equipment used in transcranial magnetic stimulation (TMS). The main working methodology adopted is the analysis of phenomena and performances in the application of the TMS procedure by creating virtual experiments, through numerical simulation. Thus, the construction and verification of computational models using the finite element method was pursued, accessible and economical in terms of computational resources, but reasonable in terms of precision, in order to be useful in technical activities in the context of TMS. As examples of applications for such models, the following can be identified: testing the viability of new solutions in the evolution of TMS equipment and CAD for their sizing; rapid comparison of performances between different models of TMS applicators; collaboration with medical personnel for the suggestive illustration of TMS principles (graphics, comparative data); choosing the settings appropriate to a certain category of interventions.

Design paths for simplified models, flexible in use, with a tendency to reduce the required computing resources, without ignoring significant quantitative aspects for the medical efficiency of the TMS procedure, were explored. In the thesis, several numerical models accessible to the user with average performance technical means (common computing technique for CAD applications) are proposed and supported by results. Starting from the analysis of a model with realistic characteristics considered as a reference in this study, the simplification of the proposed numerical models explored and evaluated directions such as: framing the problem in a certain electromagnetic regime (mode of operation), describing realistic geometry in 3D or an advantageous reduction to 2D, the option for geometric representations with more or less details, etc. These are useful economic models in engineering applications of design, verification, optimization, innovation intended for the functional improvement of medical equipment for TMS and increasing safety and comfort for the patient and practitioner. For each direction of analysis, useful conclusions were drawn in the numerical approach applied in TMS.

Chapter 1 of the paper introduces many physical, engineering and medical aspects, which come to support, on the one hand, the interest in approaching this topic and its orientation towards an interdisciplinary utility, and on the other hand to synthesize a volume of information specific to the field, important for their utilitarian character and for the scientific framing of the topic. In ***Chapter 2***, elements defining the TMS procedure as a typical application of electromagnetism are highlighted and explained through aspects such as: the generation of the inductive magnetic field, the phenomenon of electromagnetic induction applied to the production of the effective stimulus in the procedure, the operation and sizing of the electrical circuit supplying the applicator coil of the TMS equipment. Also included here are theoretical aspects: the adaptation of the theory of electromagnetism (Maxwell's equations) for TMS simulation and the quantitative definition of the stimulus itself in procedural variants of: "electrical stimulation" and respectively "magnetic stimulation" for neuronal cells.

A first study carried out within the thesis focuses on the aspects of defining numerical models for electromagnetic field analysis for simulating TMS procedures (physical and mathematical description, setting objectives, selecting the operating regime) and is systematically presented in ***Chapter 3***. The directions of idealization of the models, based on physical considerations, are critically analyzed, including by reference to benchmarks taken from the specialized literature. *Thus, a basic 3D geometric model of the human head and of a simple TMS applicator is defined, which meets sufficient elements of detail that allow the study of the procedure itself, for the clarification and control of the main physical aspects (of applied electromagnetism)*. The results highlight the correlation between the configuration of the applicator coil and the spatial distribution of the inductive magnetic field, respectively of the induced electric field and of the induced current density (affected also by the anatomical structure); also, the correlations between the time variation form of the current through the coil and the inductive magnetic field, with respect to the induced electric field and the induced current density in the cortical area, are illustrated. *It is difficult to perceive these spatial and temporal correlations at an intuitive level, although they are explained by the laws of electromagnetism; thus, the illustration through images (spectra, graphs) completes the understanding of the phenomena and provides quantitative information*. The analysis is made for the dynamic regime of the fast current pulse through the coil.

The results of this study are useful for both the technician and the physician (both concerned with aspects of the efficiency of the TMS procedure), while also having educational utility. The precision of the simulation results depends, of course, on the accuracy of the model; here, however, the anatomical details are not significant, this is not a model intended for medical applications (with therapeutic impact). The sought-after qualities are the simplicity and accessibility of the model, the rapid obtaining of results with a reasonable therapeutic character, in order to allow the extraction of information on technical aspects – for example, the performances of different applicator configurations.

The exploitation of the 3D model previously presented for TMS simulation is taken further by the study presented in ***Chapter 4*** of the paper, where a possibility of greater simplification of the computational effort is successfully explored by replacing the conditions and methods of *analysis in the time domain* (specific to the transient regime) with an approach in the *frequency domain* (if the pulse waveform is emulated by a harmonic form at a well-determined frequency). The comparison between the two approaches was made in terms of the resources involved and the results, evaluating 3D numerical models (geometry similar to the model defined and used in Chapter 3), as well as 2D idealizations (with the representation of the head based on simple geometric figures and plane-axial symmetry). The main objective was to accredit the usefulness of representing the inductor current by a harmonic waveform and from here to apply the much more economical formalism of the frequency analysis (with the representation of the equations in complex), a considerably more advantageous solution compared to the transient regime approach in the case of the pulse-shaped current. The equivalence proved to be very useful – the simulation results are very close over a useful time interval associated with the stimulation, and the savings in terms of computational resources are clearly reduced when applying the frequency analysis, provided that the harmonic regime frequency is chosen appropriately. The presentation of this solution also includes a discussion of the criteria for choosing the appropriate frequency. The chapter concludes with a comparative analysis between the two approaches conducted on different levels: evaluation of results, efficiency and consumption of computational resources, the appropriate option for a type of model depending on the specifics of the problem.

An essential aspect of this study, beyond verifying the validity of the option of replacing time analysis with frequency analysis, is the demonstration through numerical results of the qualities of the 2D geometry model; it can be successfully used in a range of TMS-related applications, with similar results to the use of the 3D model, but with much reduced resources. The comments accompanying the results precisely point out these findings.

Another study included in the thesis is the one presented in **Chapter 5** and investigates possibilities of simplified representation of the applicator structure in TMS simulation. Reducing the computational effort while maintaining the accuracy of the simulation is still an objective of the thesis. Three coil models are compared: Model (1) - a realistic coil with detailed structure at the turn level; Model (2) - an equivalent massive conductor for the entire coil; and Model (3) - a representation of the coil structure by filiform conductor. Model (1) serves as a reference point for accuracy and is the most detailed in reflecting the realistic structure. The analysis focuses on the results regarding the magnetic field distribution and the induced current density in the cortical area, compared also from the perspective of the computational effort associated with each model. The results obtained with the three models are very similar (relative differences in the margin of estimation errors) in the therapeutic application area, i.e. in the head area, and the differences decrease as the distance from the applicator increases. In conclusion, the application of the magnetic circuit law on a concrete structure shows how the magnetic field distribution (through the field spectrum and the amplitude values of the magnetic quantities) is determined by the source solenoid through the current amplitude and the spatial positioning of the conductors, less by their physical dimensions. The use of simplified representations of the conductor assembly results in significant computational savings without sacrificing accuracy, which is especially beneficial for 3D models where resource economy is critical.

Another study included in ***Chapter 5*** of the thesis investigates the effects of simplifying the head representation and the level of confidence in the viability of the results in the case of extreme simplification of the model. Within the TMS simulation, the distribution of the induced current density $\mathbf{J_{in}}$ is analyzed in two idealized 2D head models: (a) a homogeneous model and (b) a two-layer model. The results indicate that the homogeneous model overestimates the induced current levels. They are useful for objectives where the accuracy of the results is not critical, emphasizing the importance of layered models that better reflect the cranial structure for accurate bioelectromagnetic simulations.

Some side effects, which are possible when applying the TMS procedure, are highlighted in ***Chapter 6*** based on documentation from the specialized literature. Two aspects are analyzed: (1) the exposure of the patient and medical personnel to the intense magnetic field near the applicator and (2) the thermal effects associated with the electric fields induced in the body, but also in other objects exposed in the therapeutic area.

An observational study was also conducted as part of the thesis for practical application aspects of the Transcranial Magnetic Stimulation (TMS) procedure in the clinical environment; the study is presented in **Chapter 7**. Observation and analysis of the components of the real equipment used in TMS in a clinical setting provides valuable information for the numerical modeling addressed in the research program. During a demonstration at the PSIHIATRIE C&M SRL clinic, I observed the construction and functionality of the equipment together with Dr. Cosmina Mureșan, primary care psychiatrist. Trying to capitalize on both my training in the field of psychology (bachelor's studies) and the technical training through the Master's degree in Medical Engineering and doctoral studies in Electrical Engineering, my goal was to understand the practical applications and the future of TMS in psychiatric practice.

In conclusion, the results obtained in the thesis bring directions for streamlining the research process for innovating the technical infrastructure necessary in TMS – equipment with electrical, electronic, mechanical components, advanced substances and materials. The thesis proposes and evaluates simplified electromagnetic analysis models associated with the preparation and conduct of the TMS medical procedure. In this context, I have extended my training by studying several technical and bio-medical disciplines and have synthesized in the thesis the following categories and research topics:

- technical data about the equipment used and its evolution in terms of performance aspects – stimulation efficiency and safety of those involved (patient and therapist);
- medical information regarding the current spread and recognized usefulness of neuromodulation techniques within which TMS is continuously gaining ground due to its advantages;
- useful aspects in the analysis by numerical simulation for the category of electromagnetic problems addressed in the thesis, namely: a broad explanation of the sequence of physical phenomena involved in TMS technology and their understanding based on models known in physics, biophysics and electrophysiology; mathematical formalism based on the hypotheses of representing the quasi-stationary electromagnetic regime in fixed environments and non-magnetic bodies;
- aspects of numerical implementation of analysis models in the Comsol Multiphysics software environment, using the finite element method;
- complete formulation of the models and numerical analysis based on the processing of solutions and the interpretation of the results, in several studies (presented previously) having as main objective the simulation of the TMS procedure and the accreditation of simplified approach models;
- objective critical analysis followed all the simulations presented, by controlling the idealization hypotheses, by evaluating the calculation results and the consumption of computational resources.

Compared to the above synthesis of the scientific aspects included in the thesis, the following subchapter highlights the contributions that I consider original.

8.2 Original contributions

The thesis brings a series of original contributions in the field of streamlining the research process of innovative technologies used in the development of Transcranial Magnetic Stimulation (TMS) equipment.

1. The thesis includes a comprehensive synthesis based on a multidisciplinary documentary study on neuromodulation through the application of Transcranial Magnetic Stimulation techniques, to identify the main technical aspects, especially those likely to be addressed by electrical engineering (principle, equipment, simulation) through its specific research methods, such as simulation and numerical analysis in electromagnetic problems (Chapters 1 and 2).

2. A reference model for the study of TMS through numerical analysis, the finite element method, adapted for implementation in Comsol Multiphysics is formulated; the main features of the model are reviewed below.

* The computational domain (§3.2) includes a 3D inhomogeneous representation of the human head, built by adapting the geometry of a model from the Comsol library of the homogeneous head of the Specific Anthropomorphic Mannequin type, by originally completing the geometry with anatomical subdomains of the brain and eye type; for the components of the inhomogeneous domain of the head, electrical material properties for tissue media (§3.3) were assigned, taken from the international database accessible at http://niremf.ifac.cnr.it/tissprop/.

* The source of the inductive magnetic field is represented by the TMS equipment applicator, adapted in the model by a flat coil with the structure and construction inspired by the commercial products of Magstim Company Ltd., but designed for the application in the thesis, with original data; the representation for numerical modeling is through an equivalent massive coil structure, with equivalent current density, so that the provided solenoid is similar to the original one (§3.2.3).

* The calculation domain is limited to a reasonable distance in order not to affect the magnetic field distribution; accuracy verification tests were performed (§3.2.2).

* The operating mode is transient, caused by a short pulse and with a rapid increase in the current through the inductor coil, similar to typical applications (§2.1.3); it should be noted that the TMS analysis by numerical simulation is approached in the literature predominantly in the harmonic regime, and the analysis in the transient regime is rarely encountered and inconsistently documented.

3. The solution and post-processing results for the study of the TMS procedure at inductor current pulse, with the 3D numerical model described previously (see Chap. 3) qualitatively illustrate (including through suggestive images) the sequence of electromagnetic phenomena characteristic of TMS, and the set of numerical results proves the theoretically grounded, but less intuitive, connections between the electromagnetic quantities involved (§3.5.3), e.g.:

- the spatial correlation between the configuration of the applicator coil and the distribution of the inductive magnetic field, respectively the induced electric field and the induced current density (also affected by the anatomical structure);
- the temporal correlations between the time variation of the current through the coil and the inductive magnetic field, compared to the induced electric field and the induced current density in the cortical area; a very important observation, which is highlighted here but is overlooked in the analyses illustrated in the literature, shows that magnetic stimulation is effective in the first moments of the current pulse triggering through the inductive coil, regardless of the moment of reaching the maximum value of the magnetic induction – the key parameter is the rate of increase of the inductive current.

The described model is validated by the viability of its results and by their compatibility with specific TMS results published in the literature. This is the reference model for the numerical studies carried out further in the thesis and which aim to accredit models built with idealization elements (extreme simplification), in order to reduce the consumption of computing resources, but with minimal impact on accuracy.

The original elements are included in a scientific article published in the journal *Buletinul Ştiinţific UPB – series C in 2024* (Ciocăzanu, 2024). The phenomenological demonstration supported by the graphic illustration and results represents a useful educational material for explaining the TMS procedure, both for specialists in the medical field and for those in electrical engineering.

4. Another element of originality is presented in Chapter 4, through the method of equating the time domain analysis with a frequency domain analysis, namely by replacing the transient regime on the fast pulse waveform by a harmonic regime at a well-established frequency and for a short time interval, starting from the triggering of the current through the inductor coil. The frequency of the sinusoidal wave is determined by equating the initial slopes of increase of the inductor current (between the standard pulse and the sinusoid) (§4.2.3). The equivalence is valid and is supported by comparative results at the triggering of the current pulse, where the stimulation is effective (as demonstrated in Chapter 3). The advantages of this approach are:

- the results (distributions of significant field quantities) are very close, practically identical in the two approaches (§4.3.3) applied both on the model with realistic 3D geometry and on an idealized 2D model;
- considerable savings in computing resources for frequency analysis compared to time analysis (§2.2 and §4.4).

The original elements are included in a scientific article published in the journal *Revue Roumaine des Sciences Techniques, Série Électrotechnique et Énergétique in 2025* (Ciocăzanu, 2025).

5. The formulation and testing of solutions for idealizing computational models regarding simplification in the representation of the applicator - equivalent massive coil and coil made of filiform conductor - are successfully considered instead of the realistic representation of the coil with the *N* turns made of massive conductor with insulation (§5.1). The approach is illustrated in the thesis for models with 2D geometry, but the real utility is for 3D modeling in which the economy of computational resources becomes important.

6. The thesis includes a unique professional experience of the author, through the organization and implementation of an observational study in a clinic where TMS procedures are practiced. Due to bioethical restrictions, the author of the thesis did not take part in the conduct of a therapeutic intervention, but visited the specialized office, with the TMS equipment installed and functional, and had the opportunity to discuss with the specialist physician topics of professional interest, including technical data used in the thesis.

8.3 List of original publications

The published works are as follows:

1. Ciocazanu, C.-M., Stanciu, N. S., & Morega, M. (2024). „An electrical engineering perspective on neuromodulation – Characteristics of the magnetic stimulation procedure.", *U.P.B. Scientific Bulletin, Series C - Electrical engineering and Computer science, 86*(4), 349–366, *ISSN 2286-3540, eISSN 2286-3559, WOS:001380943300026*

   (online at: https://www.scientificbulletin.upb.ro/static/pdfs/full83a_737253.pdf)

2. Ciocăzanu, C.-M., Nițescu, D.-E., & Morega, M. (2025). "Useful assumption for simplified numerical analysis of transcranial magnetic stimulation / Hypothèse utile pour l'analyse numérique simplifiée de la stimulation magnétique transcrânienne.", *Revue Roumaine des Sciences Techniques, Série Électrotechnique et Énergétique,* 70(3), 427–432, *ISSN 0035-4066,* https://doi.org/10.59277/RRST-EE.2025.3.23, *WOS:001568509300001*

   (online at: https://journal.iem.pub.ro/rrst-ee/article/view/1607/607)

3. Ciocăzanu, C.-M., Niţescu, D.-E., Machedon, A., & Morega, M. (2025), „Magnetic stimulation thresholds for the perception of magnetophosphenes – a numerical study.", presented at the 14th Intl Symposium on Advanced Topics in Electrical Engineering (ATEE), Bucharest, Romania, October 9–11, 2025, proceedings indexed by IEEExplore, ISBN 979-8-3315-2646-7, *DOI:10.1109/ATEE66006.2025.11299952*

   (online at: https://ieeexplore.ieee.org/document/11299952)

8.4 Perspectives for further developments

Based on the results of this research, a significant direction for future efforts involves the increased use of the proposed simplification methods, aimed at reducing the computational time and optimizing the representation of simulation models. These methods did not focus on the clinical or medical aspects of transcranial magnetic stimulation (TMS); instead, they are intended exclusively to assist the engineering process of designing delivery coils. From this perspective, modeling and simulation strategies by simplifying models could form the basis of efficient design tools, which can provide technically sound yet computationally efficient solutions. As a result, it is possible to design coils that perform well for stimulation without the need for very complicated and time-consuming analyses. This line of research could facilitate access to easier-to-use tools for designers and accelerate the creation of TMS devices, making the engineering design process clearer, faster, and cheaper.

The thesis addressed to a limited extent the topic of side effects that may accompany the TMS medical procedure; the research program explored the idea of using the model described in the thesis to analyze the effects of stimulating the sensitive cells at the level of the retina and triggering the phenomenon of magnetophosphenes. After the stage already completed and communicated in the paper (Ciocăzanu, 2025) presented at the ATEE_2025 conference, this research direction can further capitalize on the model introduced in the thesis by extending the frequency range of the inductive magnetic field to values typical of the TMS procedure and refining the numerical model to more precisely identify the retinal area.

Another perspective for further development is oriented towards the current trend of using intelligent IT capabilities that does not bypass the field of stimulation of the nervous system, in general, and of the cerebral cortex, in particular. Between the medical technology of transcranial magnetic stimulation (TMS) and the superior IT manifestation generically called artificial intelligence (AI) there is a relationship of interconnection and mutual determination. Several ***directions of capitalizing on AI techniques and methods can be easily identified to expand the efficiency of TMS technologies*** and improve their quality (Witchalls, 2014).

On the other hand, an inverse relationship can also be identified, whereby the ***development of AI is favored by TMS technologies***, namely starting from what in modern neuroscience is called "***neuromorphic computing***", a new concept, at the same time biomimetic and evolutionary. It is a direction of hard and soft evolution of computer science, through the construction of (super)performing computing architectures, with a configuration similar to that of the central nervous system of evolved beings and emulating the way the human brain functions (Wang, 2025). On these computing systems, which are themselves built from neuromorphic materials, the implementation of AI becomes a natural and much easier process than on traditional systems (in silico).

Based on these considerations, ***directions can be identified in which TMS can, in turn, contribute to the development of AI-based computer models***, especially in the education phase.

9 Appendics - Full content of the doctoral thesis

The table of contents presents the entire content addressed in the full format of the thesis.

References (selection)

Barker, A. T., Jalinous, R., & Freeston, I. L. (1985). Non-invasive magnetic stimulation of human motor cortex. The Lancet, 325*(8437), 1106–1107.* https://doi.org/10.1016/S0140-6736(85)92413-4

Bradley, E. H., Curry, L. A., & Devers, K. J. (2007). Qualitative data analysis for health services research: Developing taxonomy, themes, and theory. Health Services Research, 42(4), 1758–1772. https://doi.org/10.1111/j.1475-6773.2006.00684.x

Brix, G., Seebass, M., Hellwig, G., & Griebel, J. (2002). Estimation of heat transfer and temperature rise in partial-body regions during MR procedures: An analytical approach with respect to safety considerations. Magnetic Resonance Imaging, 20(1), 65–76. https://doi.org/10.1016/S0730-725X(02)00483-6

Ciocazanu, C.-M., Stanciu, N. S., & Morega, M. (2024). „An electrical engineering perspective on neuromodulation – Characteristics of the magnetic stimulation procedure.", U.P.B. Scientific Bulletin, Series C - *Electrical engineering and Computer science*, 86*(4), 349–366, ISSN 2286-3540, eISSN 2286-3559, WOS:001380943300026* https://www.scientificbulletin.upb.ro/static/pdfs/full83a_737253.pdf

Ciocăzanu, C.-M., Nițescu, D.-E., & Morega, M. (2025). Useful assumption for simplified numerical analysis of transcranial magnetic stimulation / Hypothèse utile pour l'analyse numérique simplifiée de la stimulation magnétique transcrânienne. Revue Roumaine des Sciences Techniques, Série Électrotechnique et Énergétique, 70(3), 427–432. https://doi.org/10.59277/RRST-EE.2025.3.24

Ciocăzanu, C.-M., Nițescu, D.-E., Machedon, A., & Morega, M. (2025), „Magnetic stimulation thresholds for the perception of magnetophosphenes – a numerical study.", presented at the 14th Intl Symposium on Advanced Topics in Electrical Engineering (ATEE), Bucharest, Romania, October 9–11, 2025, proceedings indexed by IEEExplore, ISBN 979-8-3315-2646-7, https://doi.org/10.1109/ATEE66006.2025.11299952

Cohen, S. L., Bikson, M., Badran, B. W., & George, M. S. (2022). A visual and narrative timeline of US FDA milestones for transcranial magnetic stimulation (TMS) devices. Brain Stimulation, 15(1), 73–75. https://doi.org/10.1016/j.brs.2021.11.010

Datta, A., Elwassif, M., Battaglia, F., & Bikson, M. (2006). Bio-heat transfer model of transcranial DC stimulation: Ring vs pad electrodes. NeuroImage, 40*(1), 204–215.* https://doi.org/10.1016/j.neuroimage.2010.04.252

Di Lazzaro, V., Oliviero, A., Pilato, F., Saturno, E., Dileone, M., Tonali, P. A., & Rothwell, J. C. (2009). The physiological basis of transcranial motor cortex stimulation in conscious humans. Clinical Neurophysiology, 120*(10), 1904–1925.*

Ereifej, E. S., Parker, A. S., Heckman, P. R., & Kipke, D. R. (2019). Neural engineering: The process, applications, and its role in the future of medicine. Journal of Neural Engineering, 16(6), 063002. https://doi.org/10.1088/1741-2552/ab4869

Gomez-Tames, J., Hamasaka, A., Hirata, A., Laakso, I., Lu, M., & Ueno, S. (2020). Group-level analysis of induced electric field in deep brain regions by different TMS coils. Physics in Medicine & Biology, 65(2), 025007. https://doi.org/10.1088/1361-6560/ab5e4a

Guadagnin, V., Parazzini, M., Fiocchi, S., Liorni, I., & Ravazzani, P. (2016). Deep transcranial magnetic stimulation: Modeling of different coil configurations. IEEE Transactions on Biomedical Engineering, 63*(7), 1543–1550.*

Gutierrez, M. I., Torres, M. F., & Delgado, L. M. (2022). Advances in transcranial magnetic stimulation devices and protocols: A review of the state of the art. Frontiers in Neuroscience, 16, 865932. https://doi.org/10.3389/fnins.2022.865932

Hilli, R., Taiminen, T., Kähkönen, S., & Rimpiläinen, P. (2005). Cortical inhibition and excitability in major depressive disorder. Journal of Affective Disorders, 85*(1–2), 93–102.*

IEEE. (2019). Safety levels with respect to human exposure to electric, magnetic, and electromagnetic fields, 0 Hz to 300 GHz (IEEE Std C95.1:2019).

International Commission on Non-Ionizing Radiation Protection. (2010). Guidelines for limiting exposure to time-varying electric and magnetic fields (1 Hz to 100 kHz). Health Physics, 99*(6), 818–836.*

Karlström, E. F., Lundström, R., Stensson, O., & Hansson Mild, K. (2006). Therapeutic staff exposure to magnetic field pulses during TMS/rTMS treatments. Bioelectromagnetics, 27(2), 156–158. https://doi.org/10.1002/bem.20194

Kumsa, D. W., Bortoletto, M., & Thielscher, A. (2018). A review of computational methods for transcranial magnetic stimulation dose modeling. Brain Stimulation, 11(6), 1186–1195. https://doi.org/10.1016/j.brs.2018.07.016

Loo, C. K., & Sachdev, P. S. (2008). Transcranial magnetic stimulation in neuropsychiatry: A review of 10 years of research. Journal of Psychiatric Practice, 14*(5), 289–298.*

Lu, M., & Ueno, S. (2015). Computational study toward deep transcranial magnetic stimulation using coaxial circular coils. IEEE Transactions on Biomedical Engineering, 62*(12), 2911–2919.*

Matsumi, N., Matsumoto, K., Mishima, N., Moriyama, E., Furuta, T., Nishimoto, A., & Taguchi, K. (1994). Thermal damage threshold of brain tissue: Histological study of heated normal monkey brains. ***Neurologia Medico-Chirurgica, 34****(4), 209–215.* https://doi.org/10.2176/nmc.34.209

Riches, P. E., & Goodall, S. (2007b). Cortical voluntary activation and fatigue in older adults. European Journal of Applied Physiology, 100*(6), 603–611.*

Riches, P. E., & Houghton, G. R. (2007a). Age-related changes in central motor conduction time: A neurophysiological study. Clinical Neurophysiology, 118*(3), 450–456.*

Rotenberg, A., Horvath, J. C., & Pascual-Leone, A. (2007). The transcranial magnetic stimulation (TMS) device and foundational techniques. In Neuromethods. https://doi.org/10.1007/978-1-4939-0879-0_1

Roth, B. J. (1994). Mechanisms for electrical stimulation of excitable tissue. Critical Reviews in Biomedical Engineering, 22, 253–305.

Roth, B. J., & Basser, P. J. (1992). A model of the stimulation of a nerve fiber by electromagnetic induction. IEEE Transactions on Biomedical Engineering, 39*(6), 588–597.* https://doi.org/10.1109/10.293248

Ruohonen, J., & Ilmoniemi, R. J. (2002). Focusing and targeting of magnetic brain stimulation using multiple coils. Medical and Biological Engineering and Computing, 40*(3), 297–301.* https://doi.org/10.1007/BF02446182

Sack, A. T. (Ed.). (2023). International clinical TMS certification course – Official course materials. *Maastricht University.*

Ueno, S., & Sekino, M. (2016). Biomagnetics: Principles and applications of biomagnetic stimulation and imaging.CRC Press, Taylor & Francis Group

Wang, J., Jung, W.-B., Gertner, R. S., Park, H., & Ham, D. (2025). Synaptic connectivity mapping among thousands of neurons via parallelized intracellular recording with a microhole electrode array. Nature Biomedical Engineering. *https://www.nature.com/articles/s41551-025-01352-5*

Witchalls, C. (2014). A computer that thinks. New Scientist, 224*(2994), 28–29. https://www.aim-ahead.net/media/ptwcmyb3/ai-cares-dr-hwang.pdf*

Zibman, S., Pell, G. S., Barnea-Ygael, N., Roth, Y., & Zangen, A. (2021). Application of transcranial magnetic stimulation for major depression: Coil design and neuroanatomical variability considerations. European Neuropsychopharmacology, 45, 73–88. https://doi.org/10.1016/j.euroneuro.2021.03.004